Implementation of Forecasting-Aided State Estimation Algorithm for Distribution System Application

by

SHAHID JAMAN

Submitted to the Department of Electrical Engineering, Electronics, Computers and Systems
in partial fulfillment of the requirements for the degree of

Erasmus Mundus Master Course in Sustainable Transportation and Electrical Power Systems

at the

UNIVERSIDAD DE OVIEDO

September 2017

Author . . . .

Certified by . . . .

Dr. Jose Manuel Cano Rodriguez
Associate Professor
Thesis Supervisor

Implementation of Forecasting-Aided State Estimation Algorithm for Distribution System Application

by

SHAHID JAMAN

Submitted to the Department of Electrical Engineering, Electronics, Computers and Systems
on September, 2017, in partial fulfillment of the
requirements for the degree of
Erasmus Mundus Master Course in Sustainable Transportation and Electrical Power Systems

Abstract

State Estimation (SE) is a vital component of the Supervisory Control and Data Acquisition (SCADA) system used today in power networks. In traditional SE methods, such as Weighted Least Squares (WLS), the state variables of the grid (voltage magnitudes and phase angles) are estimated from a snapshot of the meters embedded in the network (i.e. the last measurements available). New approaches to the SE problem, known as Forecasting-Aided State Estimation (FASE), take advantage of past states in order to improve the estimation and endow the system with forecasting capabilities. The application of FASE to the low voltage grid in the context of the Smart Grid paradigm is an alluring area of research. In this work, a FASE algorithm using Kalman filters is developed and applied to a distribution network. The algorithm is implemented in Matlab and is assessed in the context of test feeders using quasi-static time series data. The performance of the new algorithm is compared with a traditional WLS implementation.

Thesis Supervisor: Dr. Jose Manuel Cano Rodriguez
Title: Associate Professor

Acknowledgments

I would like to thank Allah first for give me strength and keep me consistent to focus throughout my thesis. Then, I would like to express my heartiest appreciation to my thesis supervisor Dr. Jose Manuel Cano Rodriguez for his valuable time and kindest guidance. I feel very proud to get an opportunity of being a little part of his research team. Very special thanks to Dr. Pablo Arboleya and Md. Rejwanur Rashid Majumdar for their proper guidance and coordination. Finally, I would like to thank my family and friends who were so much supportive and motivational throughout my life.

Contents

List of Figures

List of Tables

Chapter 1

Introduction

1.1 Background

Electric power systems become complex due to the growth of demand and consumer. These complexities make the monitoring and control of power systems an important issue. The control and monitoring of the whole system are a major task of Energy Management Systems (EMS) at the control center. The state estimator, which is the valuable element of the energy management systems, provides acceptable real time data of the system state based on the available measurements on the assumed system model. The accuracy of the state estimator output should be very precise because basis on this estimation, the control center performed continuous monitoring of system conditions using telemetric data. The other actions like determination of the operating states and appropriate decision making for the preventive and corrective actions using Energy Management System (EMS) also has to be done by this estimation. The EMS functions of power depends on power flow, state estimation, security constrained unit commitment, security constrained optimal power flow etc. Thus, the state estimation process plays a significant role in ensuring the secure and economic operation of the power systems in large-scale interconnected power grids.

1.2 Introduction of SCADA in Distribution System

SCADA stands for Supervisory Control and Data Acquisition which means that the system is controlled from control center by using communication technologies. The basic function consists in estimating the state variables and performing control activity at supervisory level. The SCADA monitored system could be suitable for an oil refinery plant, a power generation and distribution system, a communication network or even a simple switching network. The SCADA collects data from the system and issue commands accordingly to monitor and control the automation system. To perform this kind of control activity, it's necessary to use different kind of sensors (Analog or Digital) and control relays. The system is supervised by a SCADA master station which collects data from monitoring devices and issues controls accordingly (either automatically or at the request of human operators) [2]

An electrical distribution system can be monitored and controlled by a SCADA system. All substations of the electricity network in a city can be controlled by SCADA system. Coordination of a power system of a country managed by SCADA central control room though the central load dispatch center and other related electricity authorities. It also manages the load demand of a city according to the power generation profile. During any emergency situation in order to avoid overall system failure, it works properly for regulation and co-ordination. The main functions of SCADA includes the power flow status within the overall system, daily and monthly power supply report and overall system operation, etc [3]

1.3 Limitation in SCADA system

In an SCADA system of a distribution network, the Remote Terminal Unit (RTU) is a very important element. RTU is used to connect sensors in the process, converting sensor signals to digital data and sending digital data to the supervisory system. The RTU connects to physical equipment. Typically, an RTU converts the electrical signals from the equipment to digital values such as voltage, current, active and reactive power. These digital values of voltage and current transmitted through a communication channel. The significant problem during this transmission is some errors added up to digital values. These errors are not only caused by the noise from AD conversion and communication issues, but also from the accuracy of the sensors (current transformers, potential transformers, etc). For this reason, after D/A conversion, we are unable to get the exact value as transmitted from RTU. This wrong value leads an SCADA system towards fault operation and control. Many researchers are working for many decades to solve this problem. State Estimation process is one of the best solutions which were accepted by many researcher and scientists. So we need an algorithm or computation tool which take the noise value and estimate the best value for power system monitoring.

1.4 Power System State Estimation Process

Power system state estimation is a process by which we can obtain the best estimate of the state of the system based on a set of measurements and the model of the system. As we know that The state of a system represents the minimum amount of information about the system at any instant of time that is necessary so that the future behavior can be determined without any information from previous instants. A state vector is a set of linearly independent variables which can provide a complete

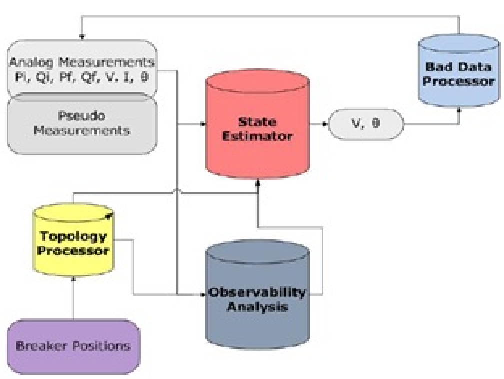

Figure 1-1: Block Diagram of basic State Estimation (SE) Process

description of the system like voltage, current, phase angle etc. A state estimator provides the state variables (voltage magnitude, phase angle), measurement error processing results, provide an estimate for all metered and unmetered quantities, filter out the small errors for all model approximation and measurements inaccuracies, detect and identify the discordant measurements which are called bad data.

1.5 Literature Review

Since the method of state estimation (SE) was first formulated and proposed [4, 5, 6] three decades ago, power system state estimation remained very plenteous and argumentative research field. As the first step of proposed method of SE, researcher selected static state estimation method [4]. This method was based on a single scan of redundant telemetry providing a time snapshot of the network. But the fact is that the demand and generation (consequently the voltage at each node) do not change drastically within the considered time frames for traditional systems. Consequently, the operators have not been concerned with the fact that the static state estimation output actually represents a 'past state'. Due to these problems, different approach or modeling of state estimation snatched researcher attention. They have proposed different kind of mathematical model and implementation of state estimation for control center[7, 8, 1]. Nowadays, as a well-performed application of EMS, the centralized single-scan weighted least squares (WLS) estimation is considered in all over the power sector. The classic performance of WLS state estimators has been done by static approach [6], where the state of the system is estimated by using a single set of measurements. It cannot predict the future operating point of the system but the accuracy of the static estimation is within acceptable limits; in other words, without using any state prediction from previous, estimations, the estimator has to be reinitialized for every new set of measurements [9]. However many different kinds of formulation has been implemented to improve WLS, such as Orthogonal Factorization, Hybrid Method, Augmented Matrix Approach, etc. [1]

In early 1970s, Dynamic State Estimators (DSE) approach provides oversimplified models to describe system state time [10, 11, 12]. Eventually, these models were unable to forecast the states. The most recent estimated state/measurement set is used as one-step ahead forecasting. Tracking estimators [13, 14, 15] were other models which followed static-state time changes. No system time evolution model is explicitly assumed by these estimators. As a result, limited forecasting skills of these models leads to state forecasting inappropriate. In [16, 17, 18] some dynamic state transition models have been proposed by introducing innovation processes which are very important method for detection and identification of anomalies (unexpected sudden changes in system state components, bad data, network configuration error etc). In this model innovation vector was defined which was the difference between forecasted and measured quantities.

More developed system state models were implemented in [19]. The proposed dynamic models were appropriate because online estimation of the parameter (using exponential smoothing and Kalman filter techniques) to adjust the models to system state time evolution. Another advanced dynamic state model with a scheme of data debugging process was proposed in [20, 21, 22]. After analyzing the computation techniques, researchers started thinking to combine all schemes like topology processor, forecasting scheme, innovation analysis, state filtering, residual analysis, data debugging etc in one algorithm. In this way, Forecasting-Aided State Estimation (FASE) has introduced in the state estimation regime.

Initially, the researchers choose Artificial Neural Network (ANN) and pattern analysis to implement DSE algorithm. So with the help of pattern analysis of raw measurements (analog or status), a real time network configuration was proposed in [22, 23]. After that papers [24, 25, 26, 27] prove that the most appropriate input variables for data debugging in ANN are normalized innovations which are better that normalized estimation residuals and raw measurements. Recently some papers [28, 29, 30, 31] supported the fuzzy control method for FASE algorithm. In these papers, they showed the comparative performance studies of their proposed FASE models and extended Kalman filter including sudden load changes.

To more attention of Forecasting-Aided State Estimation (FASE) research (some researchers also call it dynamic state estimation) some models was proposed with various Kalman filters (KF), such as extended Kalman filter (EKF) and unscented Kalman filter (UKF). The regression based state forecasting method developed in

[32] to consider fast sampling rates of voltage and phasor measurements by PMU in DSE. The predicted state was greatly improved compared with previous work and providing system operators with the capability of getting the trend in state variations. A new method using EKF based DSE was proposed in [33] to track states of a power grid. The optimum quantity and suitable locations of PMU installed in the system to ensure a satisfactory state tracking performance were discussed. In [34], a method with extension of the standard SSE based on data analysis of an electric power system using PMU was proposed. An algorithm based on the and weighting factors on the accuracy of DSE were discussed in [35]. In the paper [36, 37, 38], DSE using different measurement weighting functions was proposed to handle outliers and system sudden changes. Gaussian mixtures models were adopted in [39] to account for the stochastic characteristic of power flow in SE process. But this method is an SSE and does not have forecasting ability. In [40], a short-term load forecasting method based static SE was proposed to consider the impacts of load variations on SE. However, the DG integration was not considered.

To sum up, there are so much research activities has been already done with Dynamic State Estimation (DSE) and Forecasting-Aided State Estimation (FASE). Some researchers are continuing in this area. So the aim of this literature review is to give the complete idea about the past work on FASE and DSE. However, many missing items are very important. Following of this flow, we have tried to implement DSE algorithm and applied to a distribution system in this thesis work.

1.6 Objectives of the Master Thesis

The ultimate goal of this thesis is the implementation of a Forecasting-Aided State Estimation (FASE) algorithm. The performance of the algorithm is analyzed with respect to different factors like the variation of the smoothing constants, Mean Square Error (MSE), Mean Absolute Error (MAE), Mean Absolute Percentage Error (MAPE) and Root Mean Square Error (RMSE) etc. Then a comparison is made with conventional state estimation process (WLS) in terms of the same factor with the same distribution system. To observe the effect of optimized exponential smoothing is also an important objective of this thesis work.

1.7 Master Thesis Outline

This thesis is described in six chapters as follows:

- Chapter 1 will discuss about the basic aspects of State Estimation (SE) process in SCADA of a distribution system. It will also be discuss about the problem of SCADA system for which the monitor and control activities is possibly incorrect. Then we describe the literature review of various SE process developments. In this section, we tried to give a complete idea about the significance of FASE algorithm in distribution system state estimation (SE) process based on past research work.

- In chapter 2, it will also be shown the general formulation of Weighted Least Square (WLS) method in state estimation process. The power flow formulas, derivatives of Jacobian matrix, objective function minimization, performance indices's etc is discussed in this chapter.

- In Chapter 3, it will be shown the general modeling of Forecasting-Aided State Estimation (FASE) with Kalman filter technique. There are two well known filtering process in application of state estimation. These are Extended Kalman Filtering (EKF) Process and Unscented Kalman Filtering (UKF) Process. This work is done with EKF. It also discussed about how can be optimize the forecasting parameter to improve the forecasting in every iteration.

- In Chapter 4, the simulation result of implemented algorithm is shown in MATLAB/Simulink platform. All simulation results will be discussed based on different performance parameter. A comparative study between implemented FASE algorithm and convention WLS algorithm will also be discussed with respect to different factors. The optimized smoothing parameter effect on forecasting are also described at the end of this chapter.

- The conclusions and future work are presented in Chapter 5.

Chapter 2

Static State Estimation of Power System

The network models and complex phasor voltages of all buses are the significant elements to determine the operating state of a power system. Network operating state can be classified into six possible states with respect to various operating conditions such as secure, correctively secure, alert, controllable emergency, non-controllable emergency (in extremis), and restorative [25].

The limited equality and the inequality constraints of the network define the normal state of a power system. The equality constraints refer to the loads supplemented by the available generations. The inequality constraints state that transmission lines flows, bus voltages and generation output power must not exceed the limits [26].

2.1 Power System Security Assessment

The technical meaning of secure and correctively secure states as the normal state of a power system. In the normal state, all loads are supplied without any operating limit violations. Moreover, no violation occurs as contingency event. For instance, the system does not need any post contingency action to survive as a secure system. An outage of transmission lines or generators due to faults is the common contingencies in most of the systems. If some contingency violation occur over there and the system will need appropriate control actions to prevent loss of load due to the contingency violations, then the state is classified as 'correctively secure' [27]. In the alert state, some violations caused by a contingency cannot be corrected with any loss of load. Therefore, some preventive actions must be taken to avoid line overloading and unwanted tripping of the protection devices.

The operating condition may change significantly and operating constraints would be violated due to the lacking of preventive control actions. This state is classified as 'emergency state' and immediate corrective actions are needed by the operator to bring the system back to the alert and normal state. Lack of appropriate actions may lead the system to evolve into a 'non-controllable emergency' (in-extremis) state. In this condition, cascading of the component outages result in a partial or system-wide blackout.

The system is in the restorative state when the various loads, lines, transformers or other equipment should be disconnected to eliminate the operating constraint violations. In this stage, the system goes back to the normal state; the system would be recovered with a reduced load and reconfigured topology. The required actions to start supplying power to all the loads are referred to as 'restorative control'. The operating states and control actions in a power system are summarized in Fig 2-1.

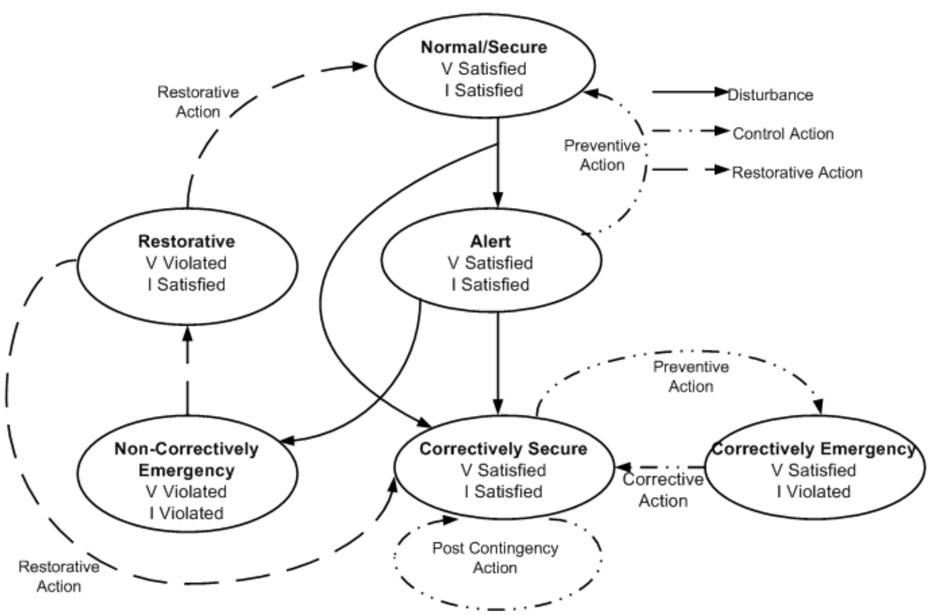

Figure 2-1: Power System State Operating Mechanism

The system run as a normal state is the ultimate goal of system operator. For this reason continuous monitoring of the system conditions is necessary to keep the grid in normal state. Consequently the operators can make appropriate decisions to take preventive or corrective actions by determining the current states. This procedure is known as 'security analyses'. Measurement acquisition is required for this analysis. A device called remote terminal units (RTU) performs the collection and transmission of various types of measurements. Normally these devices are installed in substations. Nowadays, intelligent electric devices (IED) are also used to complement the duties of RTUs. The measurements are transferred to the Supervisory Control and Data Acquisition(SCADA) host computers from all monitored substations via one of many possible types of communication links such as fiber optics, satellites, and microwaves. Figure 2-2 shows the configuration of a typical EMS/SCADA.

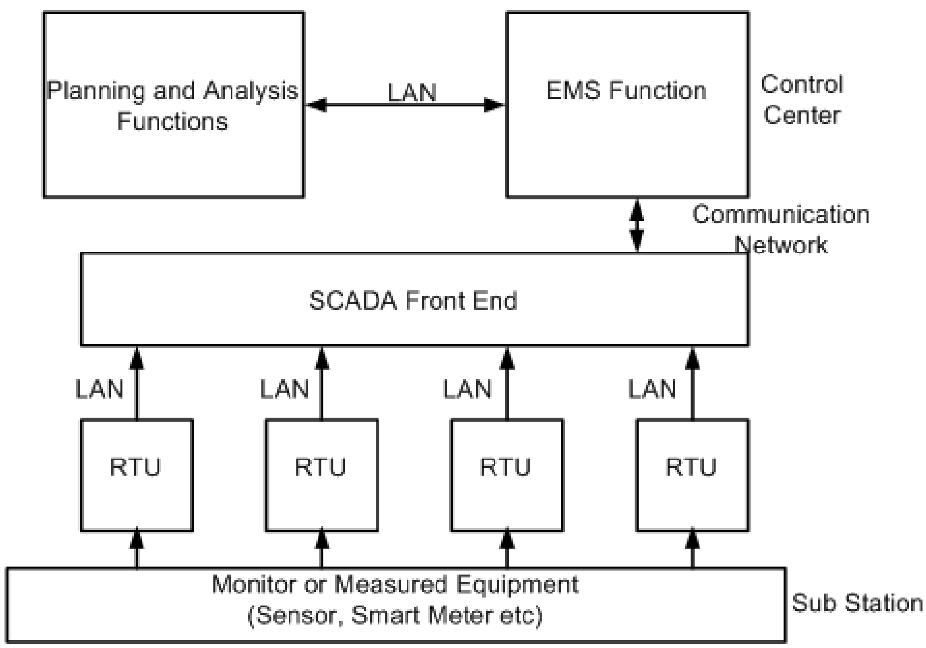

Figure 2-2: Typical EMS/SCADA configuration

The measurements includes line flows, bus voltage and line current magnitudes, generator outputs, loads, circuit breaker and switch status, transformer tap positions, and switchable capacitor bank values. A state estimator process these raw data and measurements to filter out the measurement noise and identify the total error. It gives an optimal estimate of the system by which, data center can perform various

EMS functions like contingency analysis, automatic generation control, corrective real and reactive power dispatch, load forecasting and optimal power flow to provide initial conditions. As we know that Weighted Least Square (WLS) is well accepted method of static state estimation process. In next section, WLS model, assumption, mathematical formulation are described.

2.2 Static State Estimator Modeling Methodology

The loads vary in daily operation according to pattern cycles with small variations. Sudden load changes are rarely seen and they happen due to the disconnection of big load (industrial consumers), popular TV program broadcast, scheduled outages of network components, unfavorable weather conditions, etc. Therefore, using some network parameter such as branch resistances, shunt capacitors, shunt inductor, branch reactance's and variables like bus loads, generation, nodal injection power, line flows, and bus voltages (magnitudes and phase angles), the system operating condition is fully characterized at a given point in time by consideration of quasi-static data. These co-dependent variables are related by Kirchhoff laws or so called power flow equations. Power flow equations are used to determine the line flows, and bus voltages based on the load and generation. The bus voltages are defined as 'system states' rendering the power flow equations as nonlinear. The goal of static state estimation is to provide power system operators with complex voltages (phasors) of all of the system buses at a given point in time.

2.2.1 Assumptions and Network Modeling

Firstly we assumed a balanced power system which operates in a steady-state. In balanced conditions, there are three phase branches which are fully transposed and equal load in each phase. All series or shunt devices are also in three-phase. To model correctly, we assumed single phase positive sequence circuit as 'one line diagram' for entire system. Therefore all solution given by this model is positive phase sequence component.

2.2.2 Transmission Line

A two-port π-model is used to represent the branches, whose parameters correspond to the positive sequence equivalent circuit of transmission lines. A transmission line with a positive sequence series impedance of R+jX and total line charging susceptance of jB, is modeled by the equivalent circuit shown in Figure 2-3.

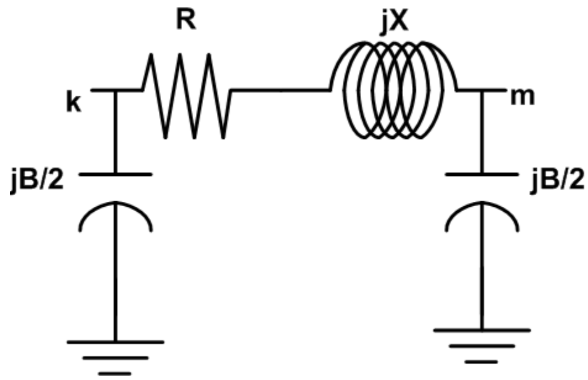

Figure 2-3: Typical pi-model of transmission lines[1]

2.2.3 Shunt Elements

The per phase susceptance represents the shunt capacitors and reactors are connected parallel to the bus. Technically shunt elements type is determined by the sign of susceptance value. Positive sign of B is a indication of shunt capacitors and for shunt reactors is vice versa.

2.2.4 Regulating Transformer and Tap Settings

We modeled a phase shifting transformer as a series impedance added with a ideal transformer of tap setting 'a' as shown in Figure 2-4.

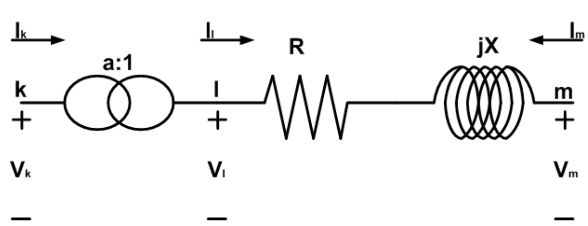

Figure 2-4: Equivalent circuit of a off nominal phase shifting transformer[1]

The terminal current injections of two port circuit given in Figure 2-4 are determined by:

$$\begin{bmatrix} i_k \\ i_m \end{bmatrix} = \begin{bmatrix} \frac{y}{a^2} & -\frac{y}{a} \\ -\frac{y}{a} & y \end{bmatrix} \begin{bmatrix} v_k \\ v_m \end{bmatrix} \tag{2.1}$$

where a is the in-phase tap ratio. The equivalent circuit for the above set of nodal equations is shown in Figure 2-5 for a phase-shifting transformer, where the off-nominal tap value a is complex, the nodal equations change to [1]:

$$\begin{bmatrix} i_k \\ i_m \end{bmatrix} = \begin{bmatrix} \frac{y}{|a|^2} & -\frac{y}{a^*} \\ -\frac{y}{a} & y \end{bmatrix} \begin{bmatrix} v_k \\ v_m \end{bmatrix} \tag{2.2}$$

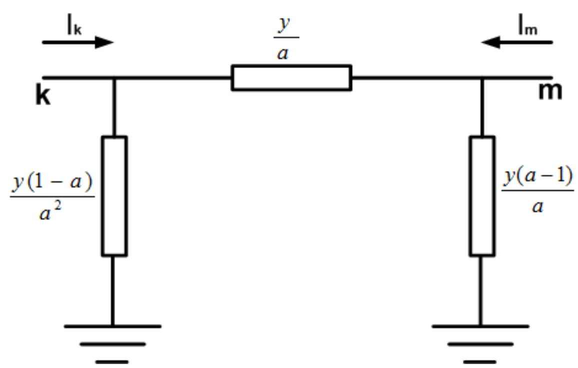

Figure 2-5: In phase tap changer equivalent circuit model.[1]

2.2.5 Generator and Loads

Constant impedance type loads are modeled as shunt admittances at the corresponding buses. Normal loads and generator are modeled as a equivalent complex power injector and therefore have no effect on the network model [1].

2.2.6 Network Mathematical Model

The network model is built based on the component models. A set of nodal equations are derived by applying Kirchhoff's current law at each bus as follows [1]:

$$\overline{I} = \begin{bmatrix} i_1 \\ i_2 \\ \vdots \\ i_N \end{bmatrix} = \begin{bmatrix} Y_{11} & Y_{12} & \cdots & Y_{1N} \\ Y_{21} & Y_{22} & \cdots & Y_{2N} \\ \vdots & \vdots & \ddots & \vdots \\ Y_{N1} & Y_{N2} & \cdots & Y_{NN} \end{bmatrix} \begin{bmatrix} v_1 \\ v_2 \\ \vdots \\ v_N \end{bmatrix} = Y^*\overline{V} \tag{2.3}$$

Where $\overline{I}$ is vector of net current injection. $\overline{V}$ represent vector of bus voltage phasor. i_k and v_k current injection and voltage phasor respectively at bus k and Y_{km} indicate $(k,m)^{th}$ element of Y. The diagonal and non-diagonal elements of bus admittance matrix are determined by following Eqn 2.4 and Eqn 2.5.

$$Y_{kk} = \sum_{m=1}^{N} y_{km} \tag{2.4}$$

$$Y_{km} = -y_{km} \tag{2.5}$$

where y_{km} is the admittance of the component connecting from bus k to bus m. The shunt components are added to the relevant diagonal terms. We can include the regulating transformer model in the admittance matrix in the following way:"

$$Y_{kk}^{new} = Y_{kk} + \frac{y}{|a|^2} \tag{2.6}$$

$$Y_{km}^{new} = Y_{km} - \frac{y}{a^*} \tag{2.7}$$

$$Y_{mk}^{new} = Y_{mk} - \frac{y}{a} \tag{2.8}$$

$$Y_{mm}^{new} = Y_{mm} + y \tag{2.9}$$

The measurement models related to the system state is given in following section.

2.3 Measurement Models

As we discussed above, the power system state is defined by the vector of phasor voltages at all the buses. The phasor angles and magnitudes are estimated as separate state variables. For a network with N buses, the state is

$$x = [\delta_2 \quad \delta_3 \quad \cdots \quad \delta_N \quad V_1 \quad V_2 \quad \cdots \quad V_N]^T \tag{2.10}$$

The phase angle of bus 1 is not consider as a state variable in Eqn 2.10 because this bus is known as slack bus and its phase angles known as 0. Each measurement z_i is uniquely calculated by a nonlinear function of the state $h_i(x)$ in the ideal case. Since measurements are not perfect, the corrupted measurements that the state estimator will process are generated by adding some error with zero mean Gaussian noise ν. The measurement model equation has given in following Eqn 2.11.

$$z = \begin{bmatrix} z_1 \\ z_2 \\ \vdots \\ z_m \end{bmatrix} = \begin{bmatrix} h_1(x) \\ h_2(x) \\ \vdots \\ h_m(x) \end{bmatrix} + \begin{bmatrix} e_1 \\ e_2 \\ \vdots \\ e_m \end{bmatrix} = h_i(x) + e_i \tag{2.11}$$

Where,

z is the measurement vector.

$h_i(x)$ is the non linear function relating i^{th} measurement to the state vector x.

$x^T = [x_1, x_2.....x_N]$ is corresponding state vector.

$h(x) = [h_1(x), h_2(x)....h_m(x)]$ is measurement vector.

$e^T = [e_1, e_2, ...e_n]^T$ is error vector associated in corrupted measurements and resulting from the limited accuracy of metering devices. Since we assumed this kind of error corresponds to white Gaussian noise with zero mean. So it has some statistical properties such as:

- $E[e_i] = 0; i = 1, 2, ...m$
- Measurement error are independent i.e $E[\nu_i \nu_j] = 0$. So it belongs to a covariance matrix with standard deviation σ_i of each measurement which reflect the expected accuracy of the corresponding meter and the communication devices. $Cov[e] = E[e_i e_j] = R$

$$R = \begin{bmatrix} \sigma_1^2 & 0 & \cdots & 0 \\ 0 & \sigma_2^2 & \cdots & 0 \\ \vdots & \vdots & \ddots & \vdots \\ 0 & 0 & \cdots & \sigma_m^2 \end{bmatrix} \tag{2.12}$$

2.3.1 Measurement Function, $h(x^k)$

Most commonly used measurements are the line power flows, bus power injections, bus voltage magnitudes and line current now magnitudes [1]. These measurements can be expressed in terms of the state variables either using the rectangular or the polar coordinates. When using the polar coordinates for a system containing N buses, the state vector will have (2N — 1) elements, N bus voltage magnitudes and (N — 1) phase angles, where the phase angle of one reference bus is set equal to an arbitrary value, such as 0. The state vector x is in the form as Eqn 2.10 assuming bus 1 is chosen as the reference. Now let us consider a general two-port π-model in Fig 2-6 for network branches, the expressions of branch components are expressed in terms of conductance and susceptance.

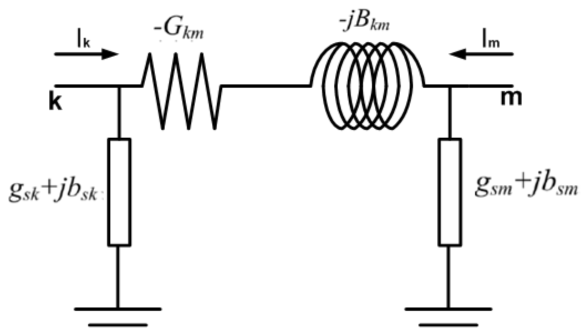

Figure 2-6: Network branch of 2-port Pi-model model.[1]

The expressions for each of the above types of measurements are given below:

- Real and reactive power injection at bus k [1]:

$$
\begin{aligned}
P_k &= V_k \sum_{m \neq k} V_m (G_{km} \cos\theta_{km} + B_{km} \sin\theta_{km}) \\
Q_k &= V_k \sum_{m \neq k} V_m (G_{km} \sin\theta_{km} - B_{km} \cos\theta_{km})
\end{aligned} \tag{2.13}
$$

- Real and reactive power flow from bus k to bus m:

$$
\begin{aligned}
P_{km} &= V_k^2 (g_{sk} + G_{km}) - V_k V_m (G_{km} \cos\theta_{km} + B_{km} \sin\theta_{km}) \\
Q_{km} &= -V_k^2 (b_{sk} - B_{km}) - V_k V_m (G_{km} \sin\theta_{km} - B_{km} \cos\theta_{km})
\end{aligned} \tag{2.14}
$$

- Line current flow from bus k to bus m:

$$
I_{km} = \frac{\sqrt{P_{km}^2 + Q_{km}^2}}{V_k} \tag{2.15}
$$

Ignoring the shunt admittance, the equation can be written as

$$
I_{km} = \sqrt{(G_{km}^2 + B_{km}^2)(V_k^2 + V_m^2 - 2V_k V_m \cos\theta_{km})} \tag{2.16}
$$

These functions represents the set of non-linear functions $h(x^k)$ that relate the state variables V_k and θ_k to the measurements. The variables in the above expressions are defined as

- V_k, θ_k are the voltage magnitude and phase angle at bus k.
- θ_{km} = θ_k - θ_m.
- $G_{km} + jB_{km}$ is the $(km)^{th}$ element of Y-bus matrix.
- $g_{km} + jb_{km}$ is the admittance of series branch between bus k and bus m. They can be calculated from line parameter by following Eqn 2.17.

$$
Y_{km} = G_{km} + jB_{km} = -y_{km} = -\frac{1}{R_{km} + jX_{km}} \tag{2.17}
$$

- $g_{sk} + jb_{sk}$ is the shunt admittance of shunt branch of bus k.

2.3.2 Measurement Jacobian, H

For a quasi-static conditions of a power system, its acceptable to linearize the function around an executing point.It can be done by Taylor series expansion, eliminating the high order elements. Once enunciate the linearization, the result is commonly named measurament Jacobian.

$$H = \frac{\partial h(x)}{\partial x} \tag{2.18}$$

The structure of Jacobian matrix can be constructed as follow:

$$H = \begin{bmatrix} \frac{\partial P_{inj}}{\partial \theta} & \frac{\partial P_{inj}}{\partial V} \\ \frac{\partial P_{flow}}{\partial \theta} & \frac{\partial P_{flow}}{\partial V} \\ \frac{\partial Q_{inj}}{\partial \theta} & \frac{\partial Q_{inj}}{\partial V} \\ \frac{\partial Q_{flow}}{\partial \theta} & \frac{\partial Q_{flow}}{\partial V} \\ \frac{\partial I_{mag}}{\partial \theta} & \frac{\partial I_{mag}}{\partial V} \\ 0 & \frac{\partial V_{mag}}{\partial V} \end{bmatrix} \tag{2.19}$$

The measurement Jacobian component corresponding to real power injection has given below[1]:

$$\frac{\partial P_k}{\partial \theta_k} = \sum_{m=1}^{N} V_k V_m(-G_{km} \sin\theta_{km} + B_{km}\cos\theta_{km}) - V_k^2 B_{kk} \tag{2.20}$$

$$\frac{\partial P_k}{\partial \theta_m} = V_k V_m(G_{km} \sin\theta_{km} - B_{km}\cos\theta_{km}) \tag{2.21}$$

$$\frac{\partial P_k}{\partial V_k} = \sum_{m=1}^{N} V_m(G_{km} \cos\theta_{km} + B_{km}\sin\theta_{km}) - V_k G_{kk} \tag{2.22}$$

$$\frac{\partial P_k}{\partial V_m} = V_k(G_{km} \cos\theta_{km} + B_{km}\sin\theta_{km}) \tag{2.23}$$

The Jacobian element corresponding to reactive power injection measurement has given below:

$$\frac{\partial Q_k}{\partial \theta_k} = \sum_{m=1}^{N} V_k V_m(G_{km} \cos\theta_{km} + B_{km}\sin\theta_{km}) - V_k^2 G_{kk} \tag{2.24}$$

$$\frac{\partial Q_k}{\partial \theta_m} = V_k V_m(-G_{km}\cos\theta_{km} - B_{km}\sin\theta_{km}) \tag{2.25}$$

$$\frac{\partial Q_k}{\partial V_k} = \sum_{m=1}^{N} V_m(G_{km}\sin\theta_{km} - B_{km}\cos\theta_{km}) - V_k B_{kk} \tag{2.26}$$

$$\frac{\partial Q_k}{\partial V_m} = V_k(G_{km}\sin\theta_{km} - B_{km}\cos\theta_{km}) \tag{2.27}$$

For real power flow, the Jacobian entries can be determine by following equations:

$$\frac{\partial P_{km}}{\partial \theta_k} = V_k V_m(g_{km}\sin\theta_{km} - b_{km}\cos\theta_{km}) \tag{2.28}$$

$$\frac{\partial P_{km}}{\partial \theta_m} = -V_k V_m(g_{km}\sin\theta_{km} - b_{km}\cos\theta_{km}) \tag{2.29}$$

$$\frac{\partial P_{km}}{\partial V_k} = -V_m(g_{km}\cos\theta_{km} + b_{km}\sin\theta_{km}) + 2(g_{km} + jg_{sk})V_k \tag{2.30}$$

$$\frac{\partial P_{km}}{\partial V_m} = -V_k(g_{km}\cos\theta_{km} + b_{km}\sin\theta_{km}) \tag{2.31}$$

The measurement Jacobian component corresponding to reactive power flow has given below:

$$\frac{\partial Q_{km}}{\partial \theta_k} = V_k V_m(g_{km}\cos\theta_{km} + b_{km}\sin\theta_{km}) \tag{2.32}$$

$$\frac{\partial Q_{km}}{\partial \theta_m} = V_k V_m(g_{km}\cos\theta_{km} + b_{km}\sin\theta_{km}) \tag{2.33}$$

$$\frac{\partial Q_{km}}{\partial V_k} = -V_m(g_{km}\sin\theta_{km} - b_{km}\cos\theta_{km}) - 2(b_{km} + jb_{sk})V_k \tag{2.34}$$

$$\frac{\partial Q_{km}}{\partial V_m} = -V_k(g_{km}\sin\theta_{km} - b_{km}\cos\theta_{km}) \tag{2.35}$$

Jacobian elements for voltage measurements at bus k can be represent by following expressions:

$$\frac{\partial V_k}{\partial \theta_k} = 0 \tag{2.36}$$

$$\frac{\partial V_k}{\partial \theta_m} = 0 \tag{2.37}$$

$$\frac{\partial V_k}{\partial V_k} = 1 \tag{2.38}$$

$$\frac{\partial V_k}{\partial V_m} = 0 \tag{2.39}$$

The Jacobian components of line current flow from bus k to bus m can be calculated by following equations:

$$\frac{\partial I_{km}}{\partial \theta_k} = \frac{g_{km}^2 + b_{km}^2}{I_{km}} V_k V_m \sin \theta_{km} \tag{2.40}$$

$$\frac{\partial I_{km}}{\partial \theta_m} = -\frac{g_{km}^2 + b_{km}^2}{I_{km}} V_k V_m \sin \theta_{km} \tag{2.41}$$

$$\frac{\partial I_{km}}{\partial V_k} = \frac{g_{km}^2 + b_{km}^2}{I_{km}} (V_k - V_m \cos \theta_{km}) \tag{2.42}$$

$$\frac{\partial I_{km}}{\partial V_m} = \frac{g_{km}^2 + b_{km}^2}{I_{km}} (V_m - V_k \cos \theta_{km}) \tag{2.43}$$

2.3.3 The Gain Matrix, $G(x^k)$

The gain matrix, G is matrix is a multiplicative form consisting Jacobian matrix,H and measurement error covariance matrix,R [1]. The measurement error covariance matrix is a diagonal matrix of measurement variances as we know from above Eqn 2.12. So the expression of gain matrix has given below:

$$G(x^k) = H^T R^{-1} H \tag{2.44}$$

$$R^{-1} = \begin{bmatrix} \frac{1}{\sigma_1^2} & 0 & \cdots & 0 \\ 0 & \frac{1}{\sigma_2^2} & \cdots & 0 \\ \vdots & \vdots & \ddots & \vdots \\ 0 & 0 & \cdots & \frac{1}{\sigma_m^2} \end{bmatrix} \tag{2.45}$$

A n-bus system has n number voltage magnitude and n-1 number of phase angles. So total number of state variables is 2n-1. If we receive m number of measurements,then the matrix of measurement error covariance matrix is $m \times m$. Hence the dimension of Jacobian matrix for n-bus is $(m) \times (2n-1)$. There the resulting dimension of gain matrix is $(2n-1) \times (2n-1)$.

The gain matrix has following properties:

- It is structurally and numerically symmetric.
- It is sparse, yet less sparse compared to R.
- In general it is a non-negative definite matrix, i.e. all of its eigenvalues are non-negative. It is positive definite for fully observable networks.

So the measurement vector $h(x^k)$ and Jacobian matrix H is most significant elements for static state estimation process. In next section, the Weighted Least Square (WLS) technique is described briefly.

2.4 Weighted Least Square (WLS) Technique

WLS estimation is useful for estimating the values of model state vector when the estimated values have various degrees of changeability over the combinations of the predictive values. Let us consider the received measurement vector is z.

$$z = [z_1, \quad z_2, \quad \cdots \quad z_m]^T \tag{2.46}$$

where m is the number of the measurements available. A non-linear function relate the measurements and the state; so no perfect measurements are considered in above Eqn 2.11.

2.4.1 Objective Function Minimization

The objective function is to minimize the sum of the squares of the weighted deviations of estimated measurements from the actual measurements. It is defined as:

$$J(x) = \sum_{k=1}^{m} \frac{(z_k - h_k(x))^2}{R_{kk}} = [z - h(x)]^T R^{-1} [z - h(x)] \tag{2.47}$$

The WLS estimator will minimized the above objective function for each state variable with respect to a threshold value [1]. At the minimum, the first order optimality will have to be satisfied. The above expression can be represent in compact form as below:

$$g(x) = \frac{\partial J(x)}{\partial x} = -H^T R^{-1} [z - h(x)] = 0 \tag{2.48}$$

2.4.2 Solution using Taylor Expansion

Using Taylor series expansion, the non-linear function $g(x)$ can be written around state vector x^k as:

$$g(x) = g(x^k) + G(x^k)(x - x^k) + ... = 0 \tag{2.49}$$

Neglecting the higher order terms leads to an iterative solution scheme known as the Gauss-Newton method.

$$x^{k+1} = x^k + [G(x^k)]^{-1} g(x^k) \tag{2.50}$$

where,

- k is the iteration index.
- x^k is solution vector at time step k.

$$G(x^k) = \frac{\partial g(x^k)}{\partial x} = H^T(x^k) R^{-1} H(x^k) \tag{2.51}$$

$$g(x^k) = -H^T(x^k) R^{-1} [z - h(x^k)] \tag{2.52}$$

We discussed about properties of gain matrix $G(x^k)$ in above section 2.3.3. Due to quite sparsity, $G(x^k)$ is not inverted so we can solve the sparsity problem by decomposing $G(x^k)$ into its triangular factors. But instead of decomposing, we can solve forward/backward substitution of following sparse linear set of equation at each iteration k.

$$[G(x^k)]\Delta x^k = H^T(x^k) R^{-1} [z - h(x^k)] \tag{2.53}$$

where,

$$\Delta x^k = x^k - [G(x^k)]^{-1} g(x^k) \tag{2.54}$$

The set of equations given by Eqn 2.53 is known as Normal Equations.

2.4.3 WLS Algorithm

Iterative solution of the Normal equations 2.53 gives the state estimation of the system. An initial guess has to be made for the state vector x^0. As in the case of power flow solution, this guess typically corresponds to the flat voltage profile, where all bus voltages are assumed to be 1.0 per unit and in phase with each other[1]. The graphical representation of WLS algorithm has given below:

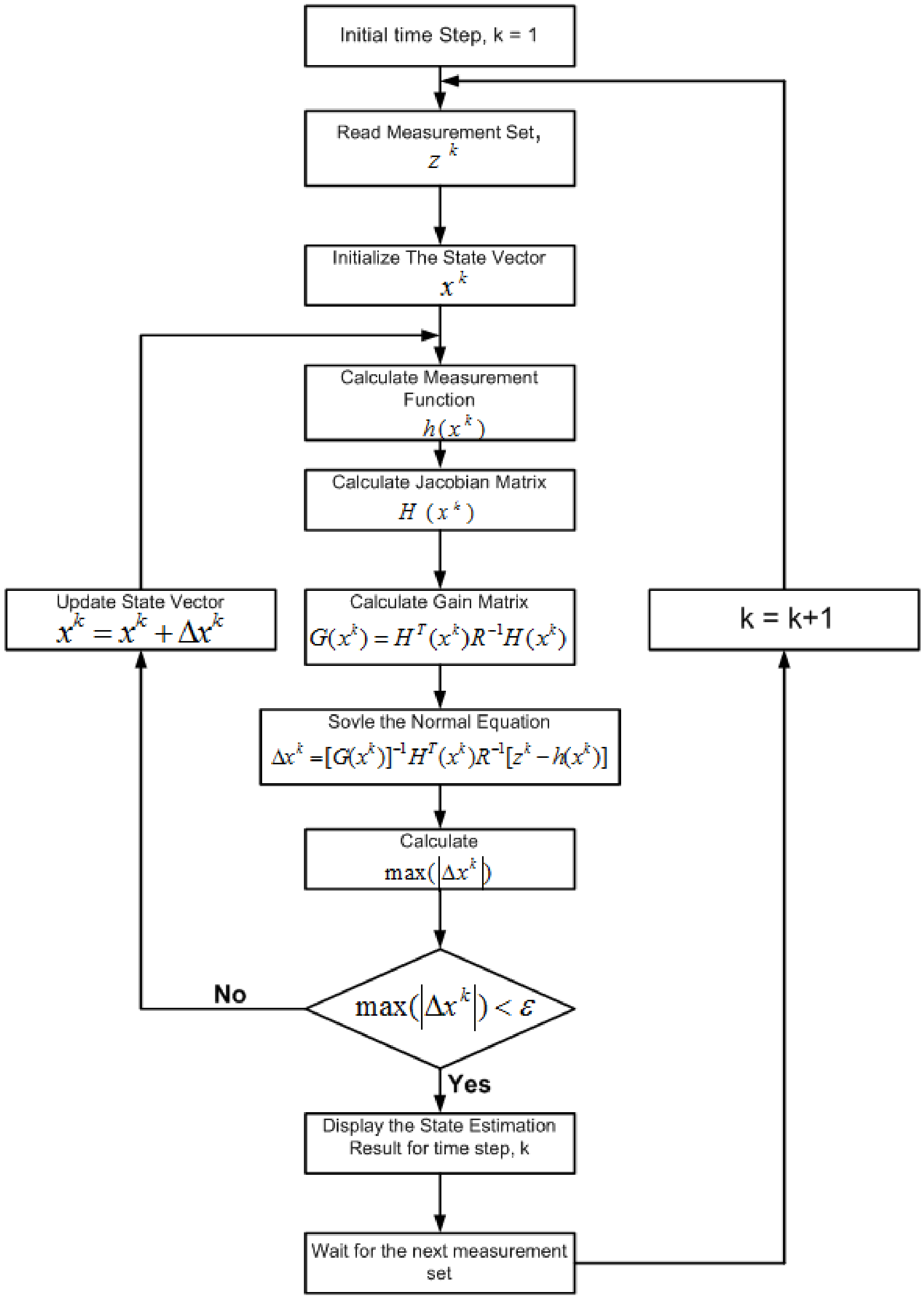

Figure 2-7: Weighted Least Square (WLS) process algorithm.

The WLS algorithm steps has given below:

1. Start the iteration by setting iteration index, k=0.

2. Initialize the state vector x^k as a flat profile.
3. Received the measurement set, z^k at iteration k.
4. Calculate the non linear measurement function vector $h(x^k)$.
5. Calculate the Jacobian matrix $H(x^k)$.
6. Calculate the Gain matrix $G(x^k)$.
7. Solve the normal equation for Δx^k from Eqn 2.53.
8. Determine the maximum absolute value among absolute Δx^k.
9. Check the convergence with a threshold value, ϵ. If it's false then update the state vector as $x^k = x^k + \Delta x^k$ and repeat the procedure from 4 with updated state vector.
10. If true then display the state estimation result and wait for next measurement set for k+1 time step.

Computational burden is the main drawback in the WLS solution algorithm that is the decomposition in triangular factors of the gain matrix or the information matrix. The constant gain matrix approximation reduces the computational burden. In WLS solution steps, flat start initialization and the converged solution of gain matrix components remain almost constant. The sensitivity of the real (reactive) power equations to changes in the magnitude (phase angle) of bus voltages are very low, especially for high voltage transmission systems [41]. Moreover, WLS method cannot capture the time-history data. Although it is known to be robust and gives satisfactory results, the main drawback is that it only considers one set of measurements. For this reason, Kalman filter based state estimation process is considered as an alternative.

Chapter 3

Forecasting Aided State Estimation

Due to the computational burden and incapability of tracking the time historic data, most researchers concentrate their efforts on dynamic state estimation technique instead of static process. The use of "Dynamic State Estimation" was noticed in [10, 28, 42] when Kalman Filter techniques were used to enhance the computational performance of the traditional WLS state estimation process in power system applications. In particular, the Kalman Filter techniques were not only used as a steady state power system model, but also to track the status of bus voltages and phase angles. At each time step, the execution of the Kalman Filter process is the inevitable part of dynamic state estimation. The computational performance was shown to be superior compared to the weighted least square (WLS) algorithm. Nowadays, DSE process with forecasting scheme is the most widely accepted technique to track the real time state variables. In this context, the Forecasting Aided State Estimation (FASE) has discussed in this chapter.

3.1 Basic Stages of FASE

Since Forecasting Aided State Estimation (FASE) is a newly research topic in the field of tracking the real time state variables, its fundamentals has FASE has are discussed in this section

3.1.1 Mathematical Modeling of FASE

The amount of information that is available for the state estimate varies depending on the particular problem has to solve [43]. So a priori and a posteriori state vector is needed for all of the measurements up to and including time k available for use in estimate of x_k. The expected value of state variable x_k before conditioning all the measurements are known as prior estimation. It is denoted as $\widetilde{x_k}$. On the other hand, the estimated value after conditioning/filtering is known as a posterior estimate. It is expressed as $\widehat{x_k}$.

The state space representation of the system based on priori estimate is given below [43]:

$$x_{k+1} = F_k x_k + g_k + w_k \tag{3.1}$$

$$z_k = h_k(x_k) + v_k \tag{3.2}$$

Where,

- k is the time sample.
- x_k is $(n \times 1)$ state vector at instant of k.
- F_k is $(n \times n)$ state transition matrix.
- g_k is the $(n \times 1)$ state trajectory associated with the trend behavior.
- w_k denotes modeling uncertainties consisting Gaussian noise with zero mean and covariance matrix Q_k i.e $N(0, Q_k)$.
- z_k represents the $(m \times 1)$ measurement vector.
- h_k denote the $(m \times 1)$ vector of non-linear measurement function of a given system which is function of state variables.
- v_k is $(m \times 1)$ Gaussian error vector consisting of Gaussian noise with zero mean and covariance matrix R_k i.e $N(0, R_k)$.

The model in Eqn 3.1 has two parameters F_k and g_k which is determined on-line by using exponential smoothing technique. This technique are discussed in section 3.3. The parameter Q_k is determined off-line by considering different operating conditions of the system.

3.1.2 State Forecasting Stage

State forecasting stage is the first part of Kalman filtering. Let us consider that an SE process has completed which gives the posterior estimate vector $\widehat{x_k}$ at the instant of k with covariance matrix P_k[43]. So for the next time step, it is possible to forecast the state vector $\widetilde{x}_{k+1}$ and its error covariance matrix M_{k+1} by performing conditional forecasting technique by using following equation.

$$\widetilde{x}_{k+1} = F_k \widehat{x}_k + g_k \tag{3.3}$$

$$M_{k+1} = F_k P_k F_k^T + Q_k \tag{3.4}$$

So using Eqn 3.3 and 3.4, we can calculate the measurement vector $\widetilde{z}_k$ and its error covariance matrix T_{k+1} by following equation.

$$\widetilde{z}_{k+1} = h_{k+1}(\widetilde{x}_{k+1}) \tag{3.5}$$

$$T_{k+1} = H_{k+1} M_{k+1} H_{k+1}^T \tag{3.6}$$

where $H_{k+1} = \frac{\partial h_{k+1}}{\partial x}$, $x = x_{k+1}$ is the Jacobian matrix. The quality of the i^{th} forecasted measurement $z_{k+1}(i)$ is represented by standard deviation $\sigma_T = \sqrt{T_{k+1}(i,i)}$.

3.1.3 Innovation Analysis Stage

Innovation analysis is a process by which we can determine the abnormality of received measurements with priori estimate. We can estimate the innovation vector $\nu_{k+1}(i)$ for i^{th} component at time instant (k+1) by difference between received measurement $z_{k+1}(i)$ and forecasted $\widetilde{z}_{k+1}(i)$. We can also calculate innovation error covariance matrix N_{k+1} using R_{k+1} and M_{k+1}.

$$\nu_{k+1} = z_{k+1}(i) - \widetilde{z}_{k+1}(i) \tag{3.7}$$

$$N_{k+1} = R_{k+1} + H_{k+1} M_{k+1} H_{k+1}^T = R_{k+1} + T_{k+1} \tag{3.8}$$

To detect the anomaly in forecasted state vector at a $k+1$ time instant, we need normalized innovations and tested its convergence with some threshold γ. The normalized vector of innovation is

$$\nu_N = \frac{|\nu(i)|}{\sigma_N(i)} \leq \gamma \tag{3.9}$$

Here, $\sigma_N(i) = \sqrt{N(i,i)}$ is the standard deviation of the innovations and the time instant notation is omitted to neglect the complexity. If at least one innovation exceeds the γ, then ν_N will be positive which means there is some abnormality in innovation vector and it should have diagnosed. Conversely ν_N will be negative for acceptable innovations and FASE algorithm will be valid for this innovation vector.

3.1.4 Kalman Filtering Stage

Kalman filter is an iterative process that exploits a set of nonlinear mathematical functions to perform estimation. It can determine the present state, even future state by the knowledge of past level and trend. The state and measurement functions are already mentioned in Eqn above 3.1 and 3.2.

Kalman filter has two major steps: Prediction and Correction (or Update). The prediction of forecasting state has already discussed in section 3.2. In this stage, the calculation of a priori state estimate which propagated to corrected stage via innovation analysis as discussed in section 3.3. The correction stage has given in the section below.

3.1.5 State Correction/Filtering Stage

In this stage, the forecasted/priori state vector $\widetilde{x}_{k+1}$ and measurement vector $\widetilde{z}_{k+1}$ can be filtered/posteriori state vector $\widehat{x}_{k+1}$ yielding with its new covariance P_{k+1}.

First of all, we have to minimize the objective function with forecasted state vector $\widetilde{z}_{k+1}$ and initial error covariance P_k. The objective function has given below

$$J(x) = [z - h(\widetilde{x}_{k+1})]^T R^{-1} [z - h(\widetilde{x}_{k+1})] + (x - \widetilde{x}_{k+1}) P_k^{-1} (x - \widetilde{x}_{k+1})^T \tag{3.10}$$

After minimization we got the acceptable forecasted state vector. Then the Kalman gain is calculated by following equation.

$$K_{k+1} = P_k H_{k+1}^T (H_{k+1}^T P_k H_{k+1} + R)^{-1} = P_k H_{k+1}^T R^{-1} \tag{3.11}$$

Finally the state vector as posteriori estimate and error covariance matrix can be updated by following equation.

$$\widehat{x}_{k+1} = \widetilde{x}_{k+1} + K_{k+1}(\widetilde{z}_{k+1} - H_{k+1}\widetilde{x}_{k+1}) \tag{3.12}$$

$$P_{k+1} = (I - K_{k+1} H_{k+1}) P_k \tag{3.13}$$

So Kalman filter working strategy is a recursive process to filtering the present and future estimate. The graphical representation of Kalman filtering process has shown in Fig 3-1 below

3.1.6 Residual Analysis Stage

A residual analysis can determine the abnormality of received measurements with posteriori estimate. It can estimate the residual vector $r_{k+1}(i)$ for i^{th} component at time instant (k+1) by difference between received measurement $z_{k+1}(i)$ and filtered $\widehat{z}_{k+1}(i)$. The residual error covariance matrix E_{k+1} using R_{k+1} and P_{k+1} can also be calculated.

$$r_{k+1} = z_{k+1}(i) - \widehat{z}_{k+1}(i) \tag{3.14}$$

$$E_{k+1} = R_{k+1} - H_{k+1} P_{k+1} H_{k+1}^T = R_{k+1} - S_{k+1} \tag{3.15}$$

To detect the anomaly in posterior state vector at a $k+1$ time instant, normalized residuals and tested its convergence with some threshold λ. The normalized vector

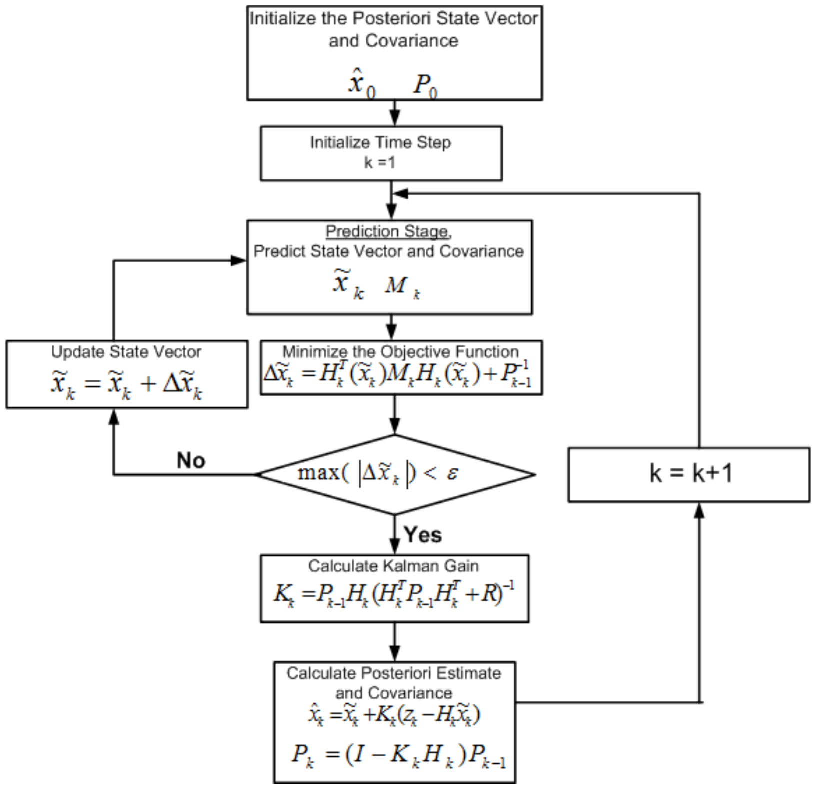

Figure 3-1: Kalman Filtering Process Algorithm

of residuals is

$$r_N = \frac{|r(i)|}{\sigma_E(i)} \leq \lambda \tag{3.16}$$

Here, $\sigma_E(i) = \sqrt{E(i,i)}$ is the standard deviation of the residuals and the time instant notation is omitted to neglect the complexity. If at least one residual exceeds the λ, then r_E will be positive which means there is some abnormality in residual vector and it should have diagnosed. Conversely r_E will be negative for acceptable residuals and FASE algorithm will be valid for this innovation vector.

3.2 FASE Algorithm

FASE is a continuous process perform but the control center, together with its EMS, is conceived as the central nervous system of the power network. The FASE algorithm flow chart has given in Fig 3-2 below.

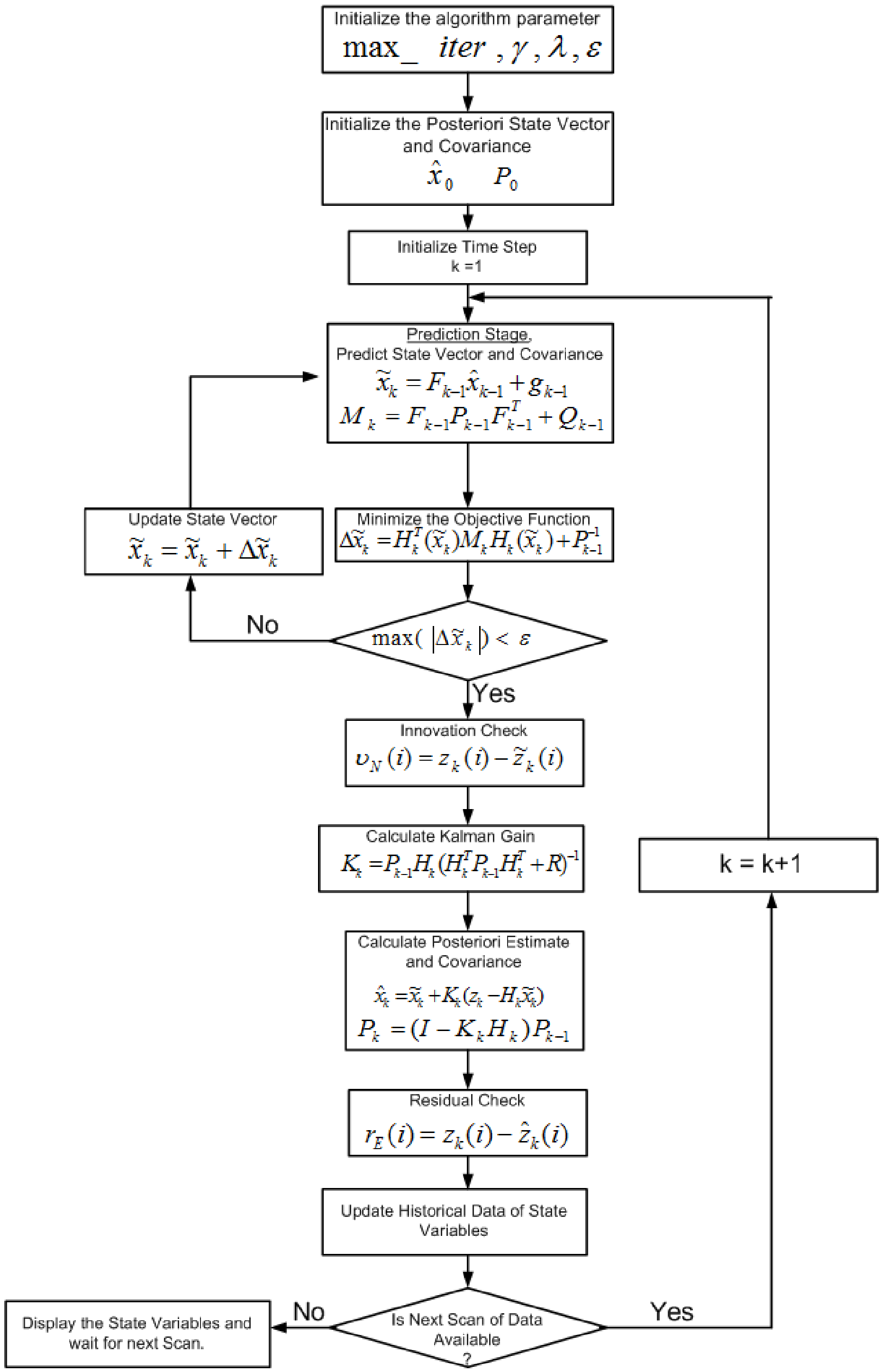

Figure 3-2: Kalman Filtering Process Algorithm

The network model is extracted From the scan of real-time data (raw measurements and status) which obtained by performing data acquisition system. The static database has the network basic topology along with electrical parameter data. In order to execute the FASE algorithm shown in Fig 3-2, some input parameters must be defined:

- max_iter is maximum number of iterations
- γ is the abnormality detection threshold for normalized innovations.
- λ is the anomaly detection threshold for normalized residuals.
- ϵ is the tolerance of estimated values, needed in the test for convergence of the filtering process.

3.3 Optimization Technique of Forecasting

As the well acceptable approach to handling the complexity of the model mentioned above in Eqn 3-1. In that equation an EKF-based method simplifies liberalizing the transit function, assuming the quasi-steady-state behavior. As we know, F_k is known as state transition matrix which determines the state vector for next time instant and g_k is the state trajectory vector defines the level and trend path for predicted state vector over the further time instants. So it is very important to determine F_k and g_k for Kalman filtering process. To optimize the FASE algorithm, we have to play with these parameters. There are many techniques already used to determine these parameters. In this thesis, we used Holt Linear Exponential Smoothing Technique. We discussed this technique in below sub section.

3.3.1 Holt Linear Exponential Smoothing

Holt's linear smoothing is a comparatively simple technique of short-term forecasting which is executable when an acceptable number of data has to be forecasted at the same time. The smoothing of the main dataset has done with its trend through two different parameters α and β whose value lying between 0 and 1. But it is noticeable in different work that the value of β followed $0 < \beta < \alpha$.

Let us consider that x_k^i is the i_{th} element of the true state vector x_k. If $\widetilde{x}_k^i$ and $\widetilde{x}_{k+1}^i$ are the predictions of state vector at time instant k and k+1 respectively, Holt's linear method expressions are

$$\widetilde{x}_{k+1}^i = a_k^i + b_k^i \tag{3.17}$$

Where a_k^i and b_k^i is the level and trend at i_{th} time instant. The level and trend equation has given below

$$a_k^i = \alpha_i x_k^i + (1 - \alpha_i)\widetilde{x}_k^i \tag{3.18}$$

$$b_k^i = \beta_i(a_k^i - a_{k-1}^i) + (1 - \beta_i)b_{k-1}^i \tag{3.19}$$

The equation 3.17 and be written as following way

$$\widetilde{x}_{k+1}^i = F_k^i \widetilde{x}_k^i + g_k^i \tag{3.20}$$

where

$$F_k^i = \alpha_i(1 + \beta_i)I \tag{3.21}$$

$$g_k^i = [(1 + \beta_i)(1 - \alpha_i)]\widetilde{x}_k^i + \beta_i a_{k-1}^i + (1 - \beta_i)b_{k-1}^i \tag{3.22}$$

where I is the identity matrix, and all associated parameters can be calculated based on a priori knowledge. Despite its rather simple implementation, this technique can offer very short-term predictions (few minutes ahead). However, this linearization step is more suited to quasi-steady-state models and may not be suitable for significant dynamic situations.

3.3.2 Performance Indices for Optimization

The forecasts should be verified or validated by comparing with historical or true data. For this validation, some performance indices are very important. There is no general agreement among researchers to determine the best process for most optimized forecasting method. But according to some research work , accuracy is the most important concern in evaluating the quality of a forecast. The goal of the forecast is to minimize error [44].

We used common indicators to evaluate accuracy particularly MAE (Mean absolute error), MSE (Mean squared error), RMSE (Root mean squared error) or MAPE (Mean absolute percentage error). We discussed the definition of these indices in the following section.

3.3.2.1 Mean Absolute Error, MAE

MAE is a indicator of overall accuracy that defines the degree of spread, where all errors are assigned equal weights.

$$MAE = \frac{1}{n}\sum_{t=1}^{n}(|e_t|) \tag{3.23}$$

Here e_t is the residuals at the time instant t. If the forecast data match with the past time series data very good, MAE is near zero, otherwise MAE is large indication of poor forecast. Thus, when two or more forecasting methods are compared, the one with the minimum MAE can be selected as most accurate [44].

3.3.2.2 Mean Squared Error, MSE

It also indicate the overall accuracy as MAE but this parameter is well acceptable in case of exponential smoothing or other techniques due to giving additional weight to large error.

$$MSE = \frac{1}{n}\sum_{t=1}^{n}(e_t)^2 \tag{3.24}$$

3.3.2.3 Root Mean Squared Error, RMSE

RMSE is a quadratic scoring rule that also measures the average magnitude of the error. It's the square root of the average of squared differences between prediction and actual observation.

$$RMSE = \sqrt{\frac{1}{n}\sum_{t=1}^{n}(e_t)^2} \tag{3.25}$$

Since the errors are squared before they are averaged, the RMSE gives a relatively high weight to large errors. This means the RMSE should be more useful when large errors are particularly undesirable.

3.3.2.4 Mean Absolute Percentage Error, MAPE

MAPE measures the deviation from the actual data in terms of percentage, that is the only difference between them. The similarity between MAE and MAPE is they both measure the absolute error.

$$MAPE = \frac{1}{n}\sum_{t=1}^{n}\frac{(|e_t|)}{x_t} \times 100 \tag{3.26}$$

3.3.2.5 Mean Absolute Scaled Error, MASE

All errors discussed before are scale dependent which means accuracy of forecasting based on relative errors. MASE is widely applicable to determine measurements forecast accuracy without the problems seen in the other measurements. This forecast evaluation statistical index is calculated for the i^{th} series of forecasted/filtered values, over a period n time samples can be calculated using Eqn 3.27 and 3.28 below:

$$MASE(i) = \frac{1}{n}\sum_{t=1}^{n}|q_t(i)| \tag{3.27}$$

$$q_t(i) = \frac{\widehat{x}_t(i) - \widetilde{x}_t(i)}{\frac{1}{t-1}\sum_{j=2}^{t}|\widehat{x}_j(i) - \widehat{x}_{j-1}(i)|} \tag{3.28}$$

The result is independent of the scale of the data. MASE can be summerized as follow:

- $MASE(i) < 1$ means the proposed forecasting methods gives smaller errors than the one step ahead forecast of naive method;
- $MASE(i) = 1$ means naive method is better than proposed forecasting technique.
- $MASE(i) > 1$ forecasts obtained with the proposed method are worse, on average than naive forecasts.

So MAD, MAPE, and RMSE are good measures, and positive and negative do not cancel each other out in either, but RMSE and MASE more aggressively punishes big errors than small ones, whereas MAD/MAPE are more linear.

3.3.3 Optimization Approach of Smoothing Constant

In contaxt of optimization of algorithm, we have to concentrate in forecasting section. The accuracy of forecasting of FASE technique depends on smoothing constant α and β. Choosing an appropriate value of exponential smoothing constant is very essential to minimize the error in forecasting.

Basically a intuition on performance indices is a method selecting a smoothing constant i, using forecast errors to guide the decision. The goal is to select a optimized smoothing constant that balances the benefits of smoothing random variations with the benefits of responding to real changes if and when they occur.

The smoothing constant sis like a weighting factor. When α is close to 1, the new forecast will include a substantial adjustment for any error that occurred in the preceding forecast. When α is close to 0, the new forecast is very similar to the old forecast.

The smoothing constant α is not an arbitrary choice but generally falls between 0.1 and 1. Low values of a are used when the underlying average tends to be stable; higher values are used when the underlying average is susceptible to change.

In practice, the smoothing constant α is often chosen by a grid search of the parameter space; that is, different solutions for a are tried starting, for example, with $\alpha = 0.1$ to $\alpha =0.9$, with increments of 0.1. The value of α with the smallest MAE, MSE, RMSE or MAPE is chosen for use in producing the good future forecasts.

Chapter 4

Case Study Simulation and Results

In this chapter, the simulation result of FASE algorithm is shown in MATLAB/Simulink platform. All simulation results discussed based on tabular and graphical format. A comparative study between our implemented FASE algorithm and conventional WLS process are also discussed with respect to different factors. Finally, the simulation results with optimized smoothing parameter is shown at the end of this chapter. The chapter starts by describing the system for which the whole case study was done.

4.1 Distribution System Description

A customer owned grid of a steelworks in the north of Spain, already tested in previous works [45] considered in this case study. The main purpose of this system is to operate some descaling pump and lightning. The system includes four tap changing transformer at between Bus 2 and 3, Bus 3 and 8, Bus 4 and 5, Bus 6 and 7. It also has buses of different voltage levels. The customer grid is connected with 220kV public utility grid through a point of common coupling (PCC). The voltage level of Bus 3 and 4 is 132kV, 30kV for Bus 5 and 6 and 13.8kV for Bus 7, 8 and 9. The grid is shown in Fig 4-1 below.

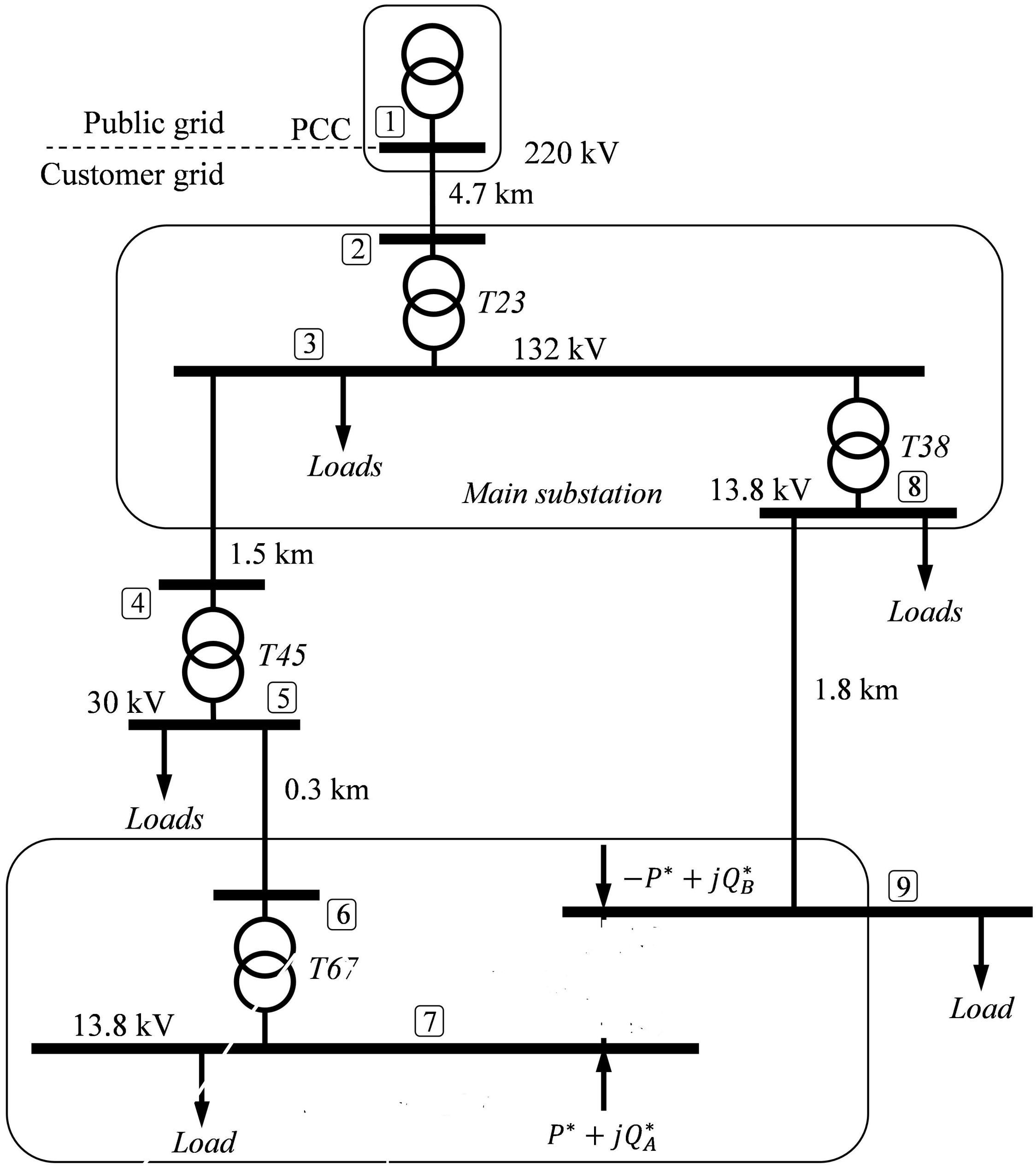

Figure 4-1: A 9 bus Industrial Distribution System in North of Spain

The parameters and configuration of the embedded transformers are listed in Table 4-1. The bus data including resistance and reactance is shown in Table 4-2. Table 4-3 depicted the lengths and per km impedances of the lines, together with the series impedances of each branch for lines and transformers. The specific power injection values considered in this case study are listed in Table 4-4.

Table 4.1: Transformer Parameters

$Transformer ID$	S_n [MVA]	R_{sc}[%]	X_{sc}[%]	a[pu]
T23	2*270	0.9	12.9	1.0125
T45	3*37.5	0.9	9	0.9875
T67	10	0.95	4.8	0.925
T38	3*50	0.92	8.5	0.975

Table 4.2: Bus Data

$BusID$	$R_{ik}[pu]$	$X_{ik}[pu]$
1	2.43×10^{-05}	2.33×10^{-04}
2	1.36×10^{-03}	2.02×10^{-03}
3	1.36×10^{-03}	1.30×10^{-04}
4	7.90×10^{-04}	7.90×10^{-03}
5	1.89×10^{-03}	4.43×10^{-04}
6	-1.46×10^{-02}	4.29×10^{-02}
7	-2.25×10^{-03}	5.08×10^{-03}
8	1.52×10^{-02}	1.06×10^{-02}

Table 4.3: Line Data

$Branch$	$Length[km]$	$R_{line}[ohm/km]$	$X_{line}[ohm/km]$
1to2	4.7	0.025	0.24
3to4	1.5	0.161	0.151
5to6	0.3	0.568	0.133
8to9	1.8	0.161	0.112

Table 4.4: Power Injections

$BusID$	$RealPower, P_i[MW]$	$ReactivePower, Q_i[MVar]$
2	0.0	0.0
3	84.0	26.0
4	0.0	0.0
5	34.0	12.0
6	0.0	0.0
7	4.9	12.6
8	52.0	39.0
9	2.7	-3.4

4.2 Data Generation as Measurement

Since the main goal of this thesis is to formulate accurate estimates for the state of the network in each time instant, the test of the estimation algorithm requires the exact state values as well as a set of measurements which would include some noise. The distribution system shown in Fig. 4.1 was solved by using the Direct Approach (DA) power flow method (See Appendix A) in order to calculate the exact state variables of the network. The solutions for 100^{th} time instant given by power flow method considered as actual state variables of each node. The state variables at the 100^{th} time instant are depicted in Table 4-5 below.

Table 4.5: State Variable from DA Power Flow Solution

$BusID$	$VoltageMagnitude, \|V\| \, [pu]$	$Angle, \angle\theta[rad]$
1	1.0000	0.0000
2	0.9997	-0.0003
3	0.9843	-0.0031
4	0.9841	-0.0031
5	0.9927	-0.0064
6	0.9921	-0.0060
7	1.0582	-0.0154
8	1.0065	-0.0057
9	0.9990	-0.0045

4.3 Corrupted or Noisy Measurement Generation

The corrupted measurements with zero means and some standard deviation is generated. In this simulation, it is assumed 0.001 standard deviation for voltages data generation and 0.02 for real and reactive power injection. This deviation added randomly with voltage, real and reactive power injections to create corrupted measurements. For example, the probability density function of real power injection at bus 2 for 100 iterations has shown in Fig 4-2 below:

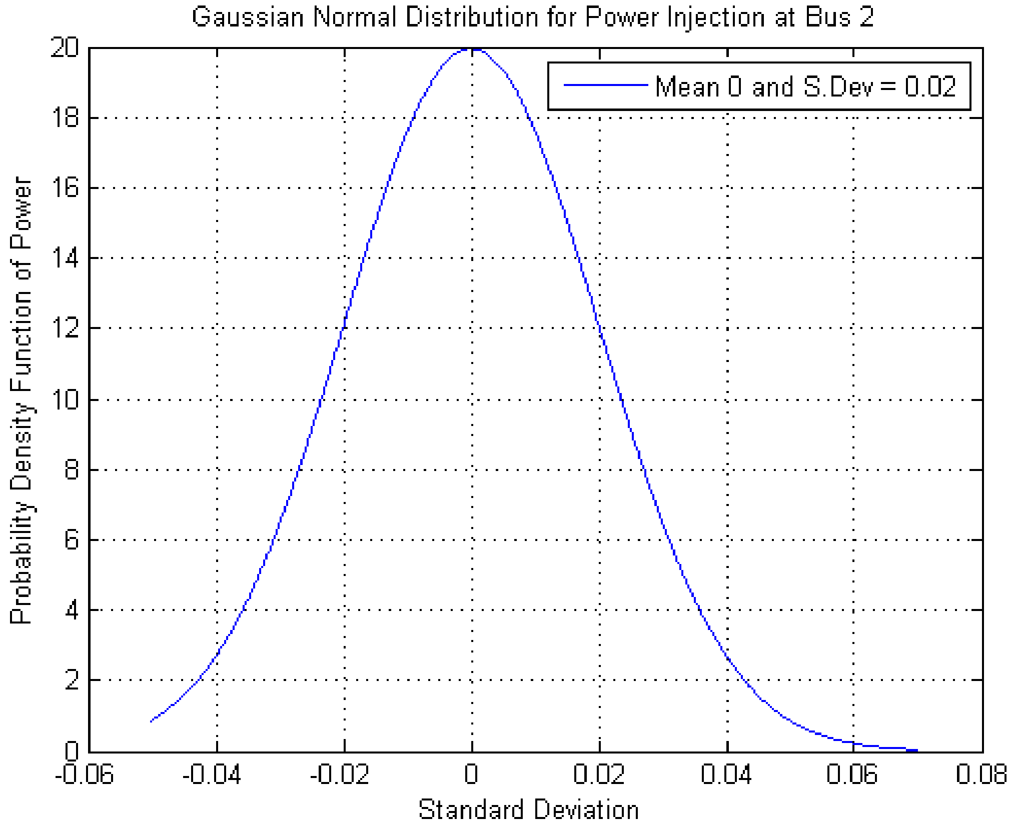

Figure 4-2: Gaussian distribution used for the generation of corrupted data for real power injection at Bus 1

Thus for this 9 bus distribution system, there are 9 voltage 8 real power and reactive power corrupted measurements generated using Gaussian probabilistic density function. For FASE process we used these measurements as a 25×1 vector Z_k. The vector structure is expressed in Eqn 4.1 below.

$$Z_k = [V_1 \quad V_2 \quad \cdots \quad V_9 \quad P_2^i \quad P_3^i \quad \cdots \quad P_8^i \quad Q_2^i \quad Q_3^i \quad \cdots \quad Q_8^i]^T \tag{4.1}$$

Here, P_2^i and Q_2^i defined as the real and reactive power injection at Bus 2.

4.4 Post Simulation Matrices and Vectors for 9 Bus System

The corrupted measurements from each node are generated. So it is possible to simulate the FASE algorithm with these measurements. After complete simulations, there are generated some important matrices which made the whole FASE process valid. The definition and dimensions of these matrices are discussed in this section.

4.4.1 Algorithm Parameters

For simulation purpose, it is necessary to define parameter constrained which has used for different conditions. The matrix parameters is showed in Table 4.6

Table 4.6: Algorithm Parameters

ParametersDefination	*Symbol*	*Value*
Total Number of Iteration	$max - iter$	100
Tolerance	tol	10^{-14}
innovation Threshold	γ	5
Residual Threshold	λ	3
Smoothing Parameter (Level)	α	0.775
Smoothing Parameter (Trend)	β	0.1

4.4.2 Posterior and Prior Vectors

Posterior and Prior vector are the most important vectors in this simulation. Posterior vector indicates the state variables after filtering process which mean the elements of this vector will display at control center of SCADA system. Similarly priori vector also express state variables but before filtering process.

$$\widehat{x}_k = [\delta_2 \quad \delta_3 \quad \cdots \quad \delta_9 \quad V_1 \quad V_2 \quad \cdots \quad V_9]^T \tag{4.2}$$

$$\widetilde{x}_k = [\delta_2 \quad \delta_3 \quad \cdots \quad \delta_9 \quad V_1 \quad V_2 \quad \cdots \quad V_9]^T \tag{4.3}$$

Here $\widehat{x}_k$ and $\widetilde{x}_k$ denoted the posteriori and priori vector at k time instant. Since the Bus 1 is slack bus, the phase angle of this bus is 0. Thus the 9 bus distribution system has 17 state variables. The dimensions of posteriori and priori vector is (17×1) column vector.

4.4.3 Jacobian Matrix

Jacobian matrix is formed based on the measurements and state variables. Each element of this matrix is in partial derivative form. Every measurement is the partial derivative with respect to each state variable.

$$H = \begin{bmatrix} \frac{\partial V_1}{\partial \theta_2} & \cdots & \frac{\partial V_1}{\partial \theta_9} & \frac{\partial V_1}{\partial V_1} & \cdots & \frac{\partial V_1}{\partial V_9} \\ \vdots & \ddots & \vdots & \vdots & \ddots & \vdots \\ \frac{\partial V_9}{\partial \theta_2} & \cdots & \frac{\partial V_9}{\partial \theta_9} & \frac{\partial V_9}{\partial V_9} & \cdots & \frac{\partial V_9}{\partial V_9} \\ \frac{\partial P_1}{\partial \theta_2} & \cdots & \frac{\partial P_1}{\partial \theta_9} & \frac{\partial P_1}{\partial V_1} & \cdots & \frac{\partial P_1}{\partial V_9} \\ \vdots & \ddots & \vdots & \vdots & \ddots & \vdots \\ \frac{\partial P_8}{\partial \theta_2} & \cdots & \frac{\partial P_8}{\partial \theta_9} & \frac{\partial P_8}{\partial V_1} & \cdots & \frac{\partial P_8}{\partial V_9} \\ \frac{\partial Q_1}{\partial \theta_2} & \cdots & \frac{\partial Q_1}{\partial \theta_9} & \frac{\partial Q_1}{\partial V_1} & \cdots & \frac{\partial Q_1}{\partial V_9} \\ \vdots & \ddots & \vdots & \vdots & \ddots & \vdots \\ \frac{\partial Q_8}{\partial \theta_2} & \cdots & \frac{\partial Q_8}{\partial \theta_9} & \frac{\partial Q_8}{\partial V_1} & \cdots & \frac{\partial Q_8}{\partial V_9} \end{bmatrix} \tag{4.4}$$

The mathematical formulation Jacobian matrix already discussed in Chapter 2. Since there are 25 measurements and 17 state variables, the dimension of the Jacobian matrix is (25×17). The observability analysis of the system can be determined by the H matrix, also known as observation matrix of the system.

4.4.4 Kalman Gain Matrix

Kalman filter quality can be determined by Kalman filter gain K. The expression of Kalman gain is shown in above Eqn 3.11 where it can be seen that this gain depends on F_k, H_k and R_k matrices. That means the Kalman gain K can be calculated off-line and saved in memory before the system operation. The dimension of Kalman gain matrix for this 9 bus system is (17×25).

The computational effort of calculating K can be saved during real-time operation by pre-computing it. If the Kalman filter is implemented in an embedded system with strict computational requirements, this can make the difference between whether or not the system can be implemented in real time. Furthermore, the performance of the filter can be investigated and evaluated before the filter is actually run. Invalidness of these matrices indicate that the algorithm wrong operation.

In summary, the matrices are different for different set of measurement received. It changes in every iteration.

4.5 Illustrative Results

The Forecasting Aided State Estimation (FASE) technique was tested in a 9-bus industrial grid. Though not conducted in this work, it would be possible to validate the algorithm in an IEEE standard distribution test network. The simulation tests were conducted using the MATLAB environment.

4.5.1 Quasi Static Load Profiles

After observing the distribution system in Fig 4-1, it is shown that there are 5 loads connected with corresponding buses 3,5,7,8 and 9. In order to emulate a quasi-dynamic behavior, a load profile is assigned to each of those loads by linking them with .csv files. These *.csv* files define the minute load profile of corresponding buses. Load profiles are defined by a matrix with two columns. The first column specifies the time, while the second column specifies the multiplier values. A portion of the Load-profile-1.csv file is shown below.

time	mult
0:01:00	0.036
0:02:00	0.036
0:03:00	0.036
0:04:00	0.036
0:05:00	0.036

Multiplier Values

Figure 4-3: Row and Columns in Load-profiles-1 csv file

The MVA value of a load at a specific time is determined by its base MVA and multiplier values. Take LOAD1 as an example, its base MVA value is 50 and the value of multiplier at time 00:01:00 is 0.036. Therefore, the MVA value of LOAD1 at time

00:01:00 is $50 \times 0.036 = 1.8$ MVA. Moreover, it is necessary to convert the appearent power into real and reactive power injection. So the KW and KVAR are calculated by assuming the power factor 0.85. Thus we can determine time series load profile for corresponding load buses. The quasi static time series load profiles are shown in Fig 4-4 below.

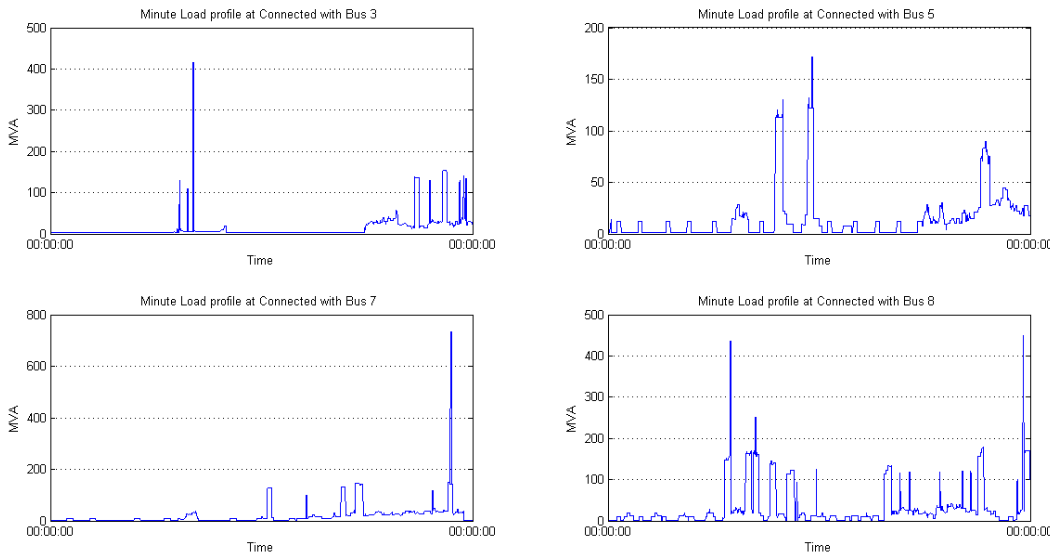

Figure 4-4: Quasi Static Time Series Load Profiles at corresponding load buses

4.5.2 Simulation Results of FASE Algorithm

A flat voltage and angle profile is considered as a posterior estimate for the initial iteration step. We have done the simulation of FASE algorithm with tolerance 10^{-14} iteratively. The voltage and angle estimate for 100^{th} time instant at the different buses as state variables of the grid are presented in Table 4-7 below.

Table 4.7: Voltage magnitudes and phase angle estimation using FASE

$BusID$	$VoltageMagnitude, \|V\| [pu]$	$Angle, \angle\theta[rad]$
1	0.9995	0.0000
2	0.9990	-0.0003
3	0.9841	-0.0032
4	0.9839	-0.0032
5	0.9926	-0.0065
6	0.9920	-0.0061
7	1.0582	-0.0155
8	1.0062	-0.0058
9	0.9987	-0.0048

A graphical representation is shown in Fig 4-5 and 4-6 below where the voltage and angle estimate of 9 buses at 100^{th} time step is very closer to the actual state variables.

The real and reactive power injection are also calculated with this estimated voltage and angles using Eqn 2.13. Table 4.8 illustrates the estimated real and reactive power injections of Bus 2 at 100^th time instant. The estimated real and reactive power injection at bus 2 over 100 iteration is plotted in Fig 4-7 and 4-8 which also matched with actual measurements.

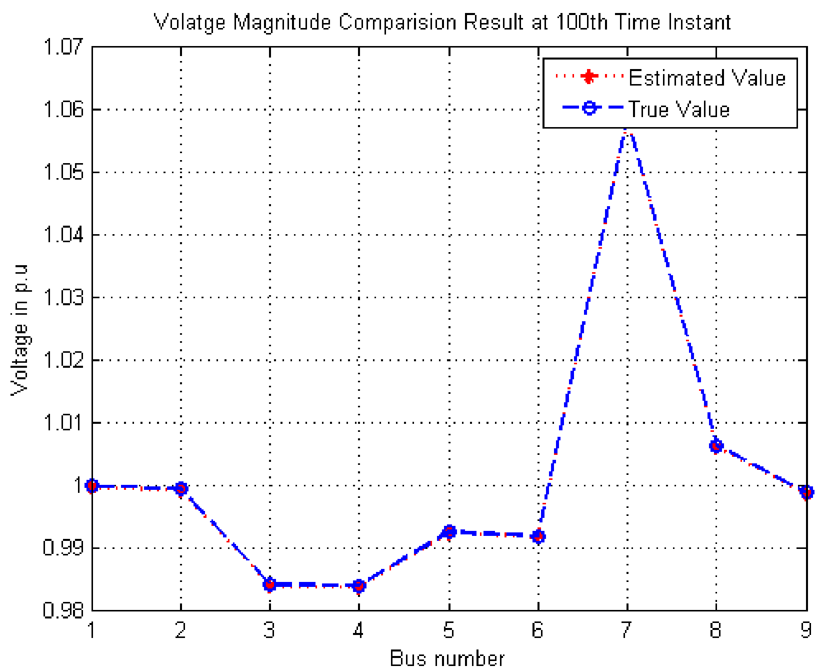

Figure 4-5: Voltage Estimation of FASE Algorithm comparing with actual voltage magnitude

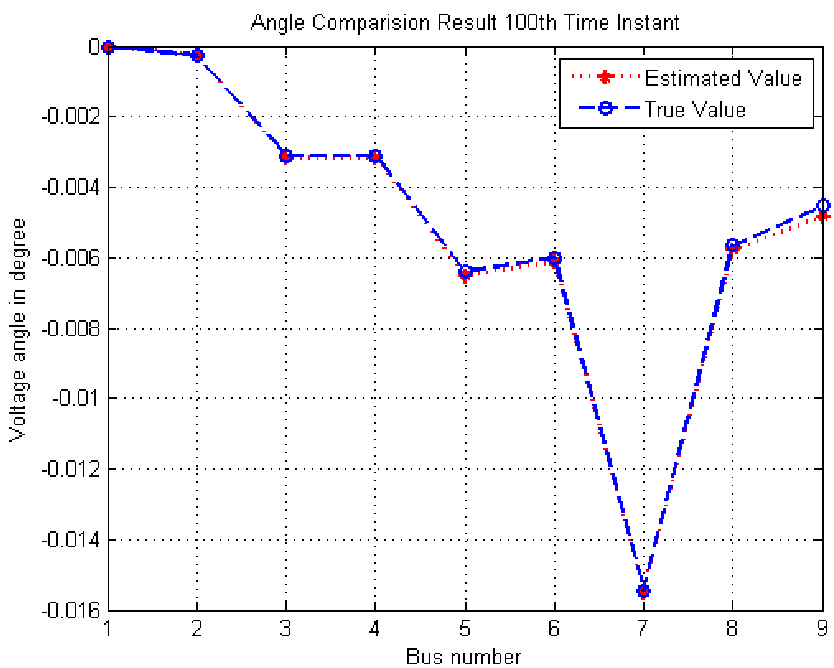

Figure 4-6: Angle Estimation of FASE Algorithm comparing with actual angle

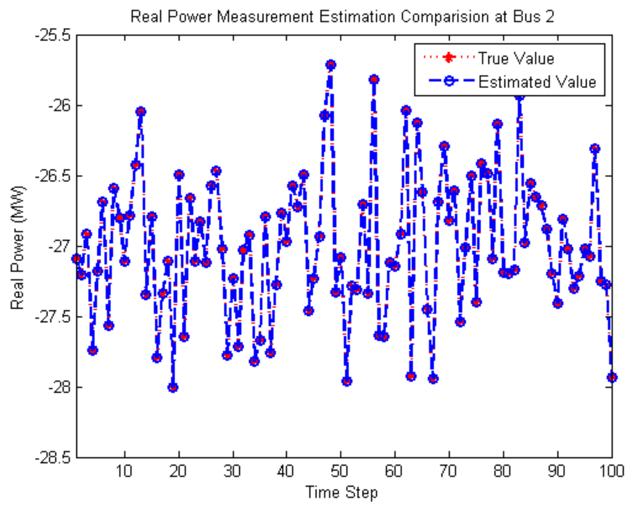

Figure 4-7: Real Power Injection Estimation over 100 iteration compared with actual measurement

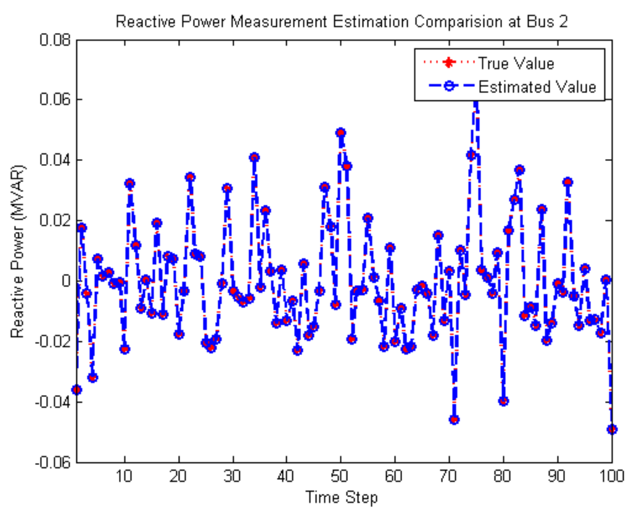

Figure 4-8: Reactive Power Injection Estimation over 100 iteration compared with actual values

Forecasting property makes FASE a more efficient and robust than any other state estimation techniques (i.e WLS). Due to forecasting, the algorithm can reach near actual state data. Thus it is very easy to estimate the state variables near the actual by the filtering process. Fig 4-9 and 4-10 depicted the forecasted and filtered state variables compared with actual. It is clearly seen that forecasted value is becoming more accurate as actual after 50 iteration.

The performance indices are very important factors to analyze the validity or ac-

Table 4.8: Real and Reactive Power Injections Comparison at 100^{th} Time Step

$BusID$	$P_{ac}[MW]$	$P_{SE}[MW]$	$Q_{ac}[MVar]$	$Q_{SE}[MVar]$
1	-0.00	-0.00	-0.00	-0.01
2	-27.0	-27.9	-25.65	-25.13
3	-0.00	-0.01	-0.00	-0.04
4	-17.50	-17.83	-16.63	-16.33
5	-0.00	-0.00	-0.00	-0.03
6	-27.50	-27.40	-25.13	-25.48
7	-21.23	-21.50	-20.42	-20.07
8	-29.84	-30.50	-28.02	-27.70
9	-0.00	-0.02	-0.00	-0.03

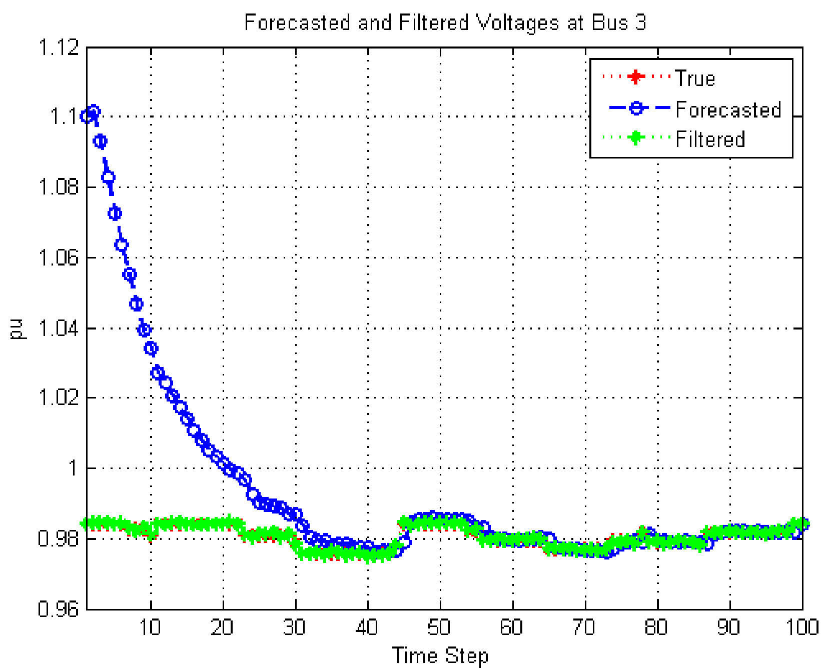

Figure 4-9: Forecasted and Filtered Voltage Magnitudes compared with actual

ceptability of state estimation technique. We discussed different types of performances in section 3.3.2 of previous chapters. Table 4.9 illustrates different performance indices for voltage magnitudes and angles of each bus. This simulation has done by considering smoothing parameter $\alpha = 0.775$ and $\beta = 0.1$.

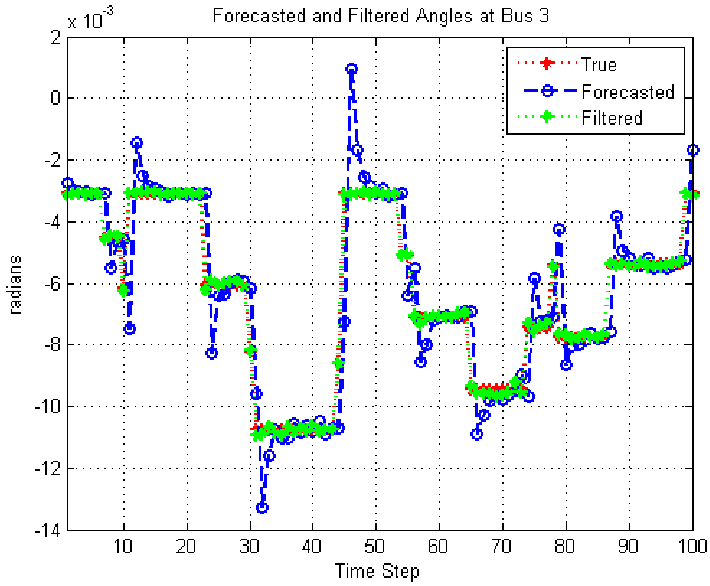

Figure 4-10: Forecasted and Filtered Angles compared with actual

Since forecasted and filtered voltage magnitudes for 9 buses and angles for 8 buses are being calculated, 100 forecasted and filtered results for voltage and angle at each bus were generated. These results are valid for specific smoothing parameter that is $\alpha = 0.775$ and $\beta = 0.1$. Using Eqn 3.23, 3.24, 3.25 and 3.26, the MAE, MSE, RMSE, and MAPE are calculated for 100 iterations. It is noticeable that different buses have different values of performance indices at specific smoothing parameter. The minimum value of that indices indicates an almost perfect estimation. For example, RMSE is minimum for Bus 1 voltage magnitude estimation for this α and β which means that this simulation is perfect for Bus 1 voltage magnitude estimation.

The performance of FASE under normal operating conditions is demonstrated through MASE indexes, calculated for all the state variables—8 time series of voltage phase angles and 9 of voltage magnitudes. The Mean Absolute Scaled Error (MASE) for this forecasting technique is depicted in Table 4.10 below.

These indexes, depicted in Fig 4-11 and 4-12 below, reveal that the adopted forecasting method presents an adequate performance, $MASE(i) < 1$ for all forecasted state time series, defeating by far the naive (tracking) method.

Table 4.9: Performance Indices of 9 Buses for $\alpha = 0.775$ and $\beta = 0.1$

Bus ID	Voltage Magnitudes				Angles			
	MAE	MSE	RMSE	MAPE	MAE	MSE	RMSE	MAPE
	($\times 10^{-4}$)	($\times 10^{-7}$)	($\times 10^{-4}$)	($\times 10^{-6}$)	($\times 10^{-4}$)	($\times 10^{-7}$)	($\times 10^{-4}$)	($\times 10^{-5}$)
1	2.90	1.30	2.90	2.91	-	-	-	-
2	2.89	1.28	3.58	2.78	5.24	3.24	5.69	1000
3	2.72	1.14	3.37	2.89	58	393	62.7	920
4	2.71	1.13	3.36	2.77	0.64	0.075	0.866	9.80
5	2.60	1.10	3.31	2.64	59	456	67.55	472.3
6	2.61	1.10	3.32	2.65	6.72	7.27	8.52	61.2
7	4.76	4.65	6.81	4.64	160	4050	201.22	552.7
8	2.84	1.33	3.64	2.86	139	3600	189.78	1228.1
9	3.55	2.26	4.75	3.65	29	131	36.21	296.7

Table 4.10: Forecast Errors of Bus Voltages Magnitudes and angles

$BusID$	$MASE, \|V\|\,[pu]$	$MASE, \angle\theta[rad]$
1	0.0001219	-
2	0.0002228	0.0000007
3	0.0001233	0.0000065
4	0.0001234	0.0000062
5	0.0001281	0.00001359
6	0.0001281	0.00001314
7	0.0001539	0.00001314
8	0.0001324	0.00001427
9	0.0001452	0.00001274

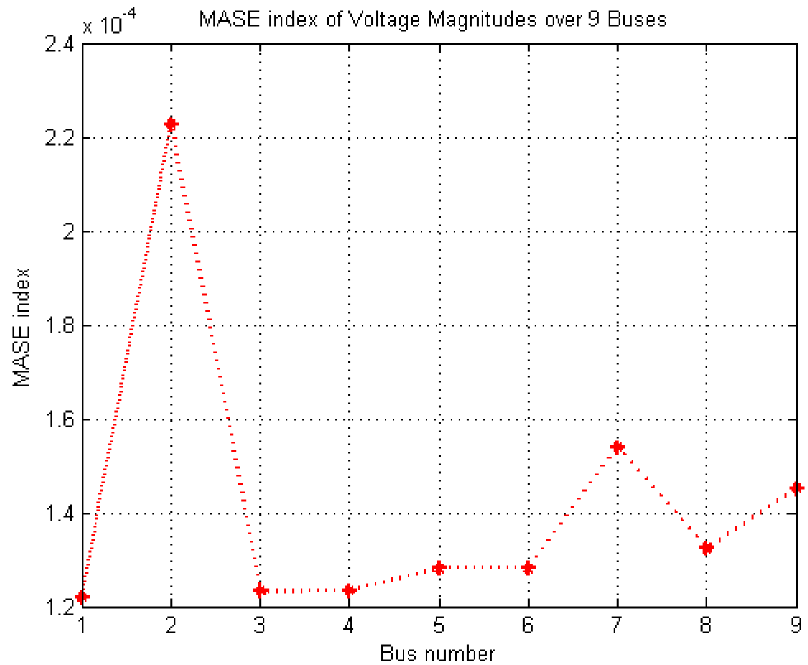

Figure 4-11: Forecast error measure for Bus Voltage Magnitudes

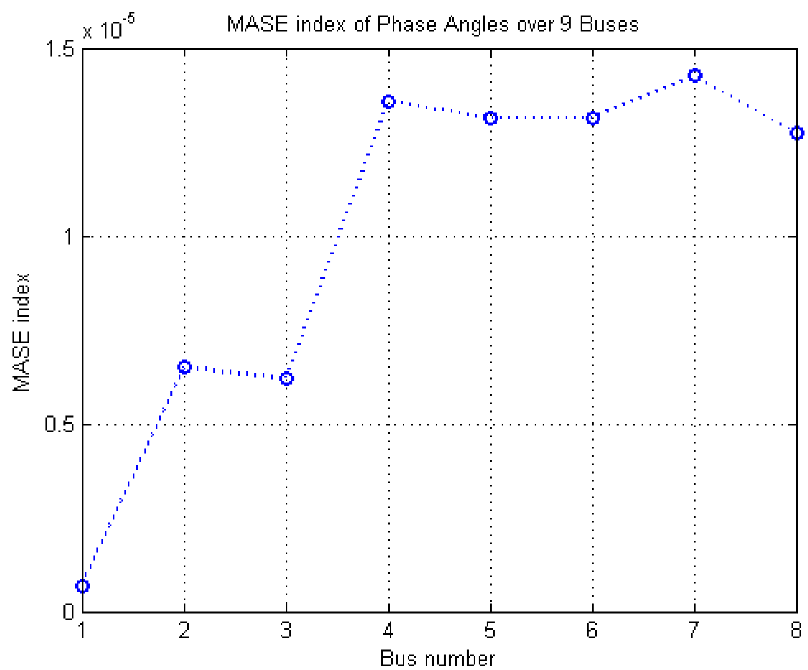

Figure 4-12: Forecast error measure for Bus Phase Angles

4.6 Comparative Study between FASE and WLS Techniques

As it is well-known, Weighted Least Square (WLS) method is well established and globally accepted method of state estimation. Any other approach to the field, then, should confront its results towards this well-accepted algorithm. Forecasting Aided State Estimation is a new technique, it is a mandatory task to make a comparison study with WLS to validate its accuracy. If the result of FASE is closer or similar to actual values, thus FASE algorithm has worked and estimated correctly. A comparative study is discussed in this section.

The results of both FASE and WLS methods are compared and simulated with respect to same actual values. It is used the same measurements in both case. The only difference is in state estimation techniques. The state variables estimation of both methods is shown below.

Table 4.11: Voltage Magnitude Comparison of 9 Buses

Bus ID	Voltage Magnitudes		Angles	
	FASE	WLS	FASE	WLS
	pu	pu	rad	rad
1	0.9998	0.9998	0	0
2	0.9995	0.9995	-0.0003	-0.0003
3	0.9841	0.9841	-0.0032	-0.0031
4	0.9839	0.9839	-0.0032	-0.0031
5	0.9926	0.9926	-0.0065	-0.0064
6	0.9920	0.9920	-0.0061	-0.0060
7	1.0582	1.0582	-0.0155	-0.0155
8	1.0063	1.0063	-0.0058	-0.0057
9	0.9987	0.9987	-0.0048	-0.0046

So the state variable estimation using FASE is valid. Because this technique giving almost same result as WLS. The graphical representation of these results is shown in Fig 4-13 and 4-14.

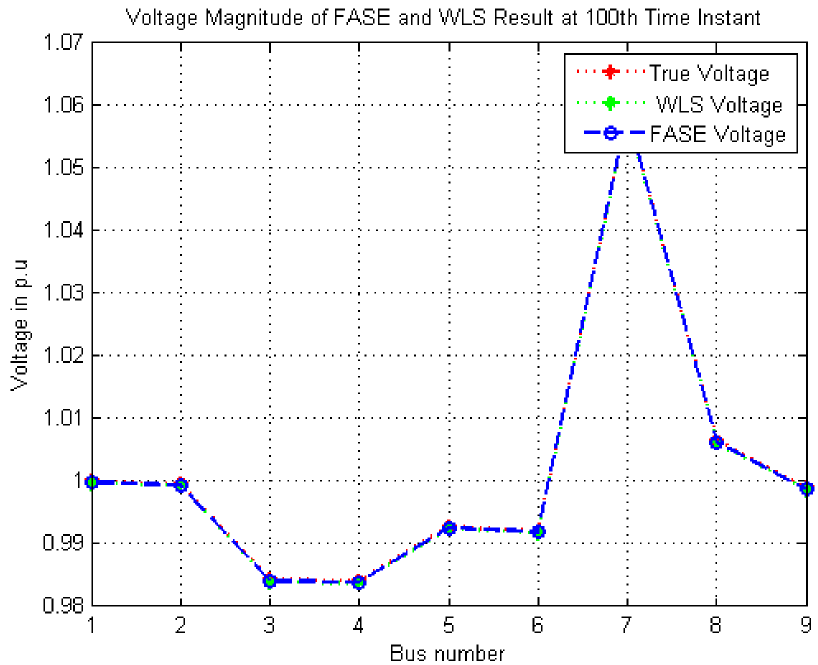

Figure 4-13: Voltage Magnitudes of FASE and WLS comparing with Actual Value

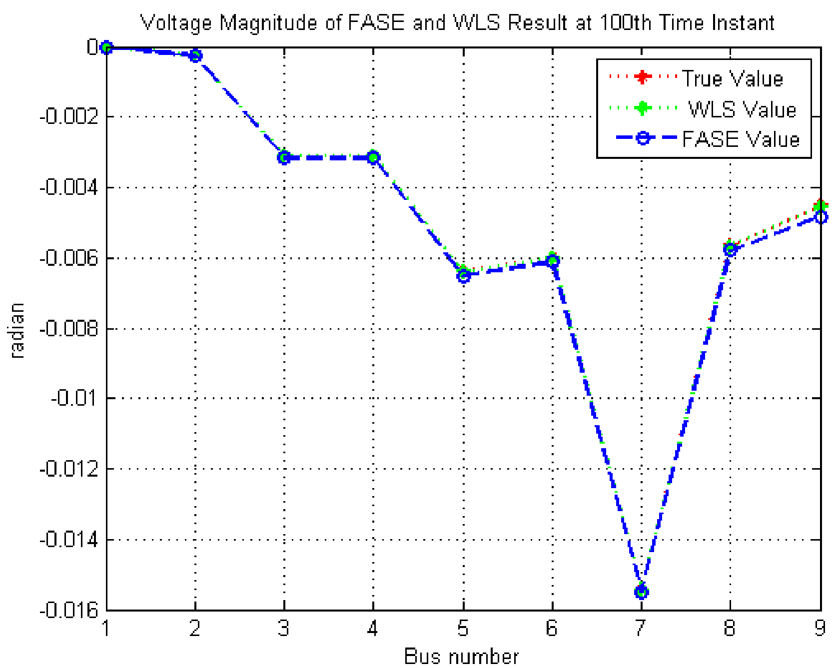

Figure 4-14: Phase Angles of FASE and WLS comparing with Actual Value

It can be proved that the real and reactive power injections of the 9 buses, calculated from the estimated state variables, are very close to the actual values.

Table 4-12 is illustrating that numerical results.

Table 4.12: Comparison of Real and Reactive Power Injection Estimation

Bus ID	Real Power Injection		Reactive Power Injection	
	FASE	WLS	FASE	WLS
	kW	kW	kVar	kVar
1				
2	0.00	-0.01	0.01	0.09
3	-27.93	-27.09	-25.69	-25.65
4	0.02	0.18	-0.05	-0.49
5	-18.19	-17.57	-16.14	-16.58
6	-0.01	-0.10	-0.01	-0.10
7	-27.29	-27.48	-25.84	-26.10
8	-21.67	-21.52	-20.64	-20.45
9	-30.29	-29.58	-27.35	-27.96

These results indicate that FASE has a good prediction and estimation capability which can be used as an alternative of WLS method. Real and reactive power comparison for 9 buses after 100 iterations is shown in Fig 4-15 and 4-16 below.

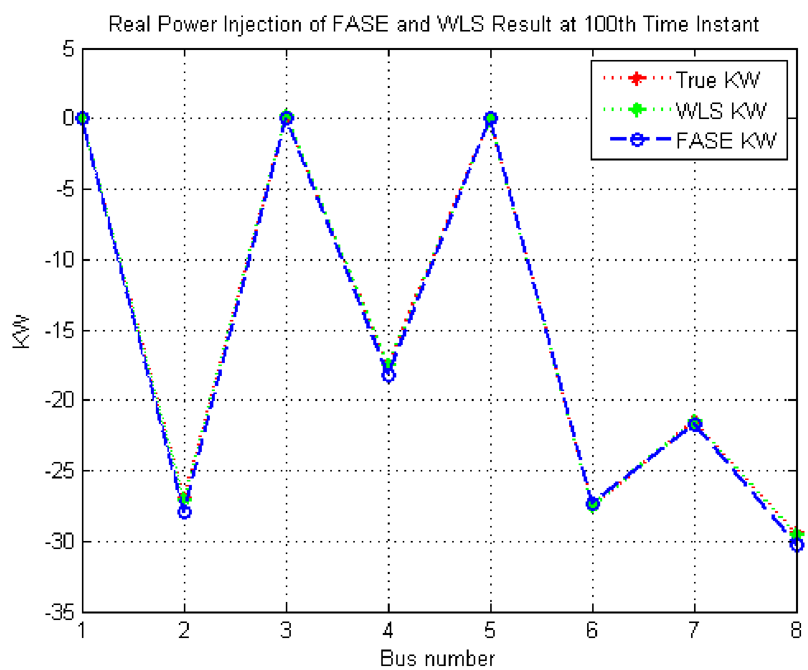

Figure 4-15: Real Power Injections of FASE and WLS comparing with Actual Value

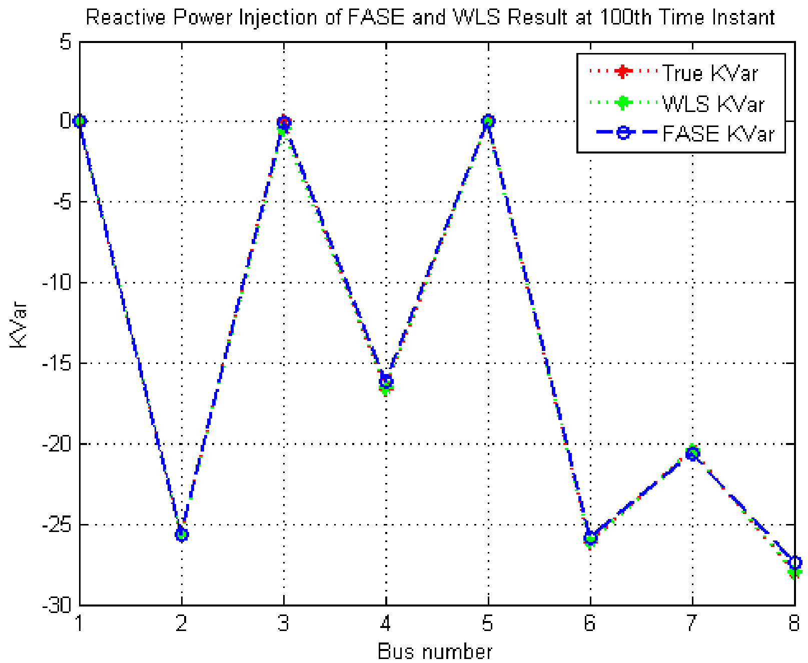

Figure 4-16: Reactive Power Injections of FASE and WLS comparing with Actual Value

To measure the accuracy between FASE and WLS method, it is necessary to observe the performance indices for both cases. Less value of performance indices indicates less estimation error. Table 4.13 and 4.14 depict the performance indices for voltage and angle.

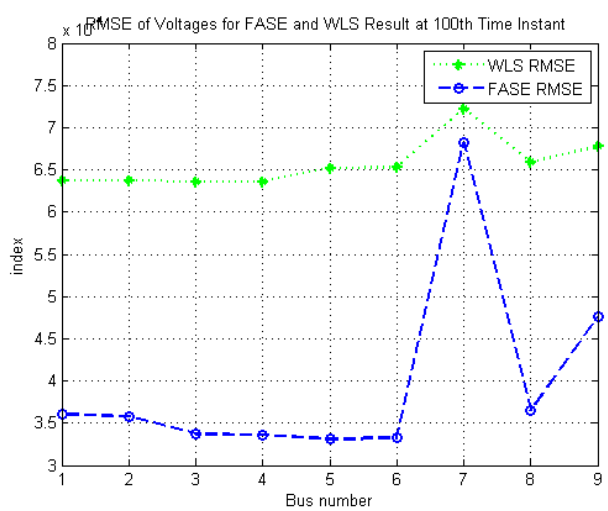

Figure 4-17: RMSE of Voltage Mangitudes for FASE and WLS

Table 4.13: Performance Indices of Voltage Magnitudes for 9 Buses

Bus ID	Voltage Magnitudes of 9 Buses							
	MAE		MSE		RMSE		MAPE	
	FASE	WLS	FASE	WLS	FASE	WLS	FASE	WLS
	10^{-4}	10^{-4}	10^{-7}	10^{-7}	10^{-4}	10^{-4}	10^{-6}	10^{-6}
1	2.91	5.013	1.29	4.059	3.61	6.371	2.913	5.012
2	2.90	5.015	1.28	4.065	3.58	6.376	2.899	5.018
3	2.72	4.983	1.137	4.039	3.37	6.356	2.779	5.083
4	2.72	4.985	1.131	4.041	3.36	6.358	2.774	5.086
5	2.60	5.093	1.098	4.254	3.31	6.523	2.642	5.169
6	2.61	5.098	1.104	4.264	3.32	6.531	2.650	5.180
7	4.76	5.617	4.647	5.215	6.82	7.222	4.630	5.397
8	2.85	5.147	1.33	4.347	3.65	6.593	2.850	5.166
9	3.55	5.255	2.261	4.593	4.76	6.778	3.650	5.393

Table 4.14: Performance Indices of Phase Angles for 9 Buses

Bus ID	Phase Angles of 9 Buses							
	MAE		MSE		RMSE		MAPE	
	FASE	WLS	FASE	WLS	FASE	WLS	FASE	WLS
	10^{-4}	10^{-4}	10^{-7}	10^{-7}	10^{-4}	10^{-4}	10^{-5}	10^{-5}
1								
2	5.25	5.24	3.24	3.23	5.69	5.69	1000.00	1000.00
3	57.71	57.67	393.16	392.16	62.70	62.62	916.50	916.50
4	0.64	0.13	0.08	0.00	0.87	0.17	9.80	2.18
5	0.64	58.87	456.25	451.50	67.55	67.19	472.35	472.73
6	6.73	6.80	7.26	7.42	8.52	8.62	61.15	60.59
7	159.65	159.48	4049.08	4004.04	201.22	200.10	552.71	553.77
8	138.58	138.68	3601.47	3613.38	189.78	190.09	1228.11	1229.68
9	28.95	28.80	131.13	125.66	36.21	35.45	296.71	292.44

From the above table, we are observing the different types of errors for 9 buses in case of voltage magnitudes and phase angles. According to the MAE, MSE, RMSE, and MAPE of voltage magnitudes, it is clearly seen that the FASE is a better technique than WLS for voltage magnitude estimation. All errors for FASE are lower than WLS. However, the amount of error in both cases is very small which means FASE is very good estimation method as WLS. For phase angle, errors are also almost same that the WLS algorithm. The graphical representation of RMSE for voltage magnitudes and phase angles is shown in Fig 4-17 and 4-18.

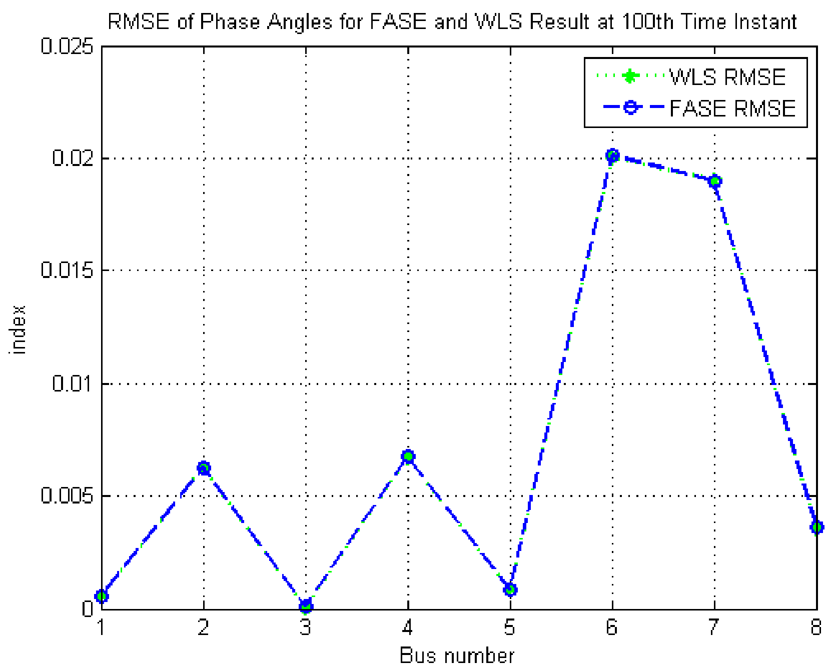

Figure 4-18: RMSE of Phase Angles for FASE and WLS

The voltage estimation error over 100 iterations is also shown in Fig 4-19 which also depict that the amount of error is negligible between the two techniques. The real and reactive power injection estimation from FASE also has less error over estimation period. It also can be observed that the relative errors also reduced after 50 iteration in case of FASE estimation because the priori estimate is improving after that iteration. The level and trend parameters replace the previous data in every iteration, which is also a cause of the reduction of the estimation error.

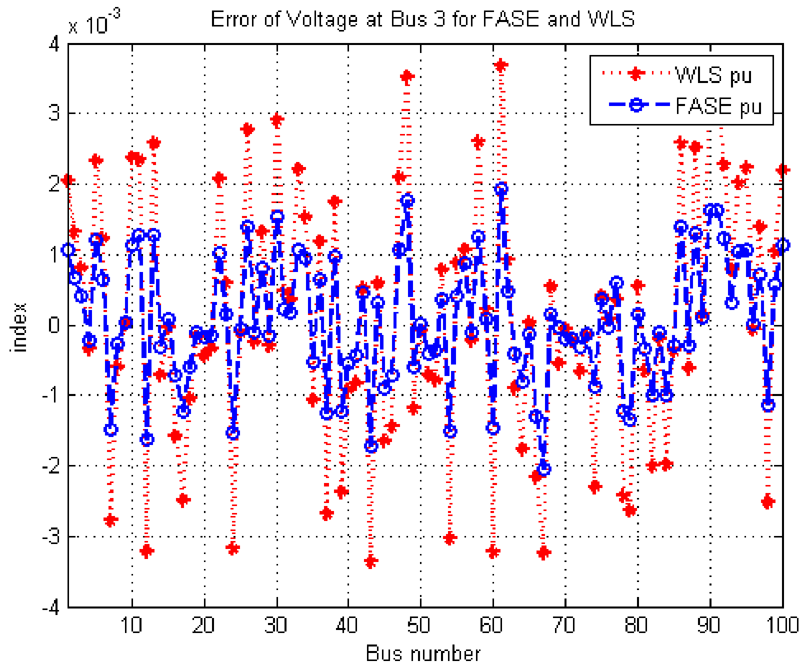

Figure 4-19: Voltage Estimation Error for FASE and WLS over 100 iteration

It can be seen an insignificant difference between the estimated state of FASE and WLS method. Remark: it should be noted that for WLS method, the inverse matrix J must be calculated for each iteration, until reaching the prescribed tolerance; while in the simulation with Kalman filter, this inverse is calculated just once, so the computational effort is reduced undoubtedly.

4.7 Effect of Optimized Smoothing Parameters on Forecasting

Different values of the smoothing constants would be tried out on past data; the best ones would minimize some chosen measure of error. The assumption is that these constants will continue to perform well in the future. As we know from section 3.3, it is not possible to forecast a certain series of data without a fixed level and trend smoothing parameter α and β. The performance indices like MAE, MSE, RMSE and MAPE are determined for the given series of data with parameters α and β. But a fixed value of smoothing constant is not a good parameter to forecast different series of data. The best value of α and β should be different to forecast of different series of data. So it is possible to make an improved forecast by playing with this two smoothing variables α and β.

There are 17 state variables in the system and it is simulated the FASE algorithm for 100 iterations, every state variable should have different set of data with 100 elements or every state variable has (1×100) row vector. So there is a possibility to have different optimal α and β pair for each set of data. In this section, the effect of smoothing parameter variation on forecast and also tried to determine the best value of smoothing parameter which can give the best forecast. The smoothing of a specific dataset was done with its trend through two different parameters α and β whose value lying between 0 and 1. But it is noticeable in different work that the value of β followed $0 < \beta < \alpha$ [43].

With this flow, we determined the optimum α and β for state variable forecast at each node which is listed in Table 4-15. In this table, we choose the smoothing parameter based on MSE and RMSE performance indices.

Table 4.15: Optimum α and β for improved state variable forecast

Voltage Magnitudes	α	β	Phase Angles	α	β
V_1	0.7	0.179	θ_1	-	-
V_2	0.7	0.179	θ_2	0.7	0.1
V_3	0.775	0.189	θ_3	0.925	0.1
V_4	0.925	0.211	θ_4	1	0.221
V_5	0.925	0.1	θ_5	0.775	0.1
V_6	0.925	0.1	θ_6	0.85	0.2
V_7	0.925	0.1	θ_7	0.85	0.1
V_8	1	0.221	θ_8	0.7	0.257
V_9	0.925	0.211	θ_9	0.775	0.189

Table 4-16 are illustrating the performence indices for different α and β which calculated the data of voltage magnitude forecast at Bus 2.

Table 4.16: Performance Indices at Different α and β for Voltage Magnitude Node 2

α	β	MAE	MSE	RMSE	MAPE
		10^{-4}	10^{-7}	10^{-4}	10^{-6}
0.7	0.100	144.0	105.0	324.0	135.0
0.7	0.179	2.637	1.0572	3.252	2.639
0.7	0.257	2.740	1.1509	3.392	2.742
0.7	0.336	2.838	1.2552	3.543	2.840
0.7	0.414	2.950	1.3744	3.707	2.952
0.7	0.493	3.062	1.5077	3.883	3.064
0.7	0.571	3.195	1.6534	4.066	3.198
0.7	0.650	3.349	1.8135	4.259	3.351
0.775	0.100	2.666	1.1016	3.319	2.668
0.775	0.189	2.796	1.2128	3.482	2.798
0.775	0.279	2.927	1.3356	3.655	2.929
0.775	0.368	3.061	1.4760	3.842	3.063
0.775	0.457	3.201	1.6318	4.040	3.204
0.775	0.546	3.360	1.8043	4.248	3.363
0.775	0.636	3.535	1.9954	4.467	3.538
0.775	0.725	3.724	2.2064	4.697	3.727
0.85	0.10	2.844	1.2723	3.567	2.846
0.85	0.20	3.003	1.4144	3.761	3.005
0.85	0.30	3.159	1.5740	3.967	3.161
0.85	0.40	3.319	1.7535	4.187	3.321
0.85	0.50	3.503	1.9548	4.421	3.505
0.85	0.60	3.698	2.1798	4.669	3.701
0.85	0.70	3.908	2.4308	4.930	3.911
0.85	0.80	4.140	2.7099	5.206	4.143
0.925	0.100	3.062	1.4876	3.857	3.064
0.925	0.211	3.232	1.6643	4.080	3.234
0.925	0.321	3.410	1.8682	4.322	3.413
0.925	0.432	3.612	2.0996	4.582	3.615
0.925	0.543	3.832	2.3611	4.859	3.835
0.925	0.654	4.081	2.6561	5.154	4.084
0.925	0.764	4.344	2.9880	5.466	4.347
0.925	0.875	4.615	3.3614	5.798	4.619
1	0.100	3.298	1.7494	4.183	3.300
1	0.221	3.492	1.9715	4.440	3.494
1	0.343	3.720	2.2337	4.726	3.723
1	0.464	3.969	2.5336	5.033	3.972
1	0.586	4.235	2.8760	5.363	4.238
1	0.707	4.515	3.2668	5.716	4.519
1	0.829	4.804	3.7125	6.093	4.808
1	0.950	5.100	4.2224	6.498	5.104

So from the above Table, it is found that to give a best forecast of voltage magnitude at node 2, it is choosen $\alpha = 0.7$ and $\beta = 0.179$ because the performance indices are minimum at this α and β. Optimized α pair can give a good forecast than other pair. Fig 4-20 and 4-21 depicted the effect of optimized α and β on state variable forecasting at Bus 2. It is clear from the figure that forecasting has improved for optimum smoothing parameter. For a good forecast of phase angle at Bus 2, we have to choose $\alpha = 0.925$ and $\beta = 0.1$.

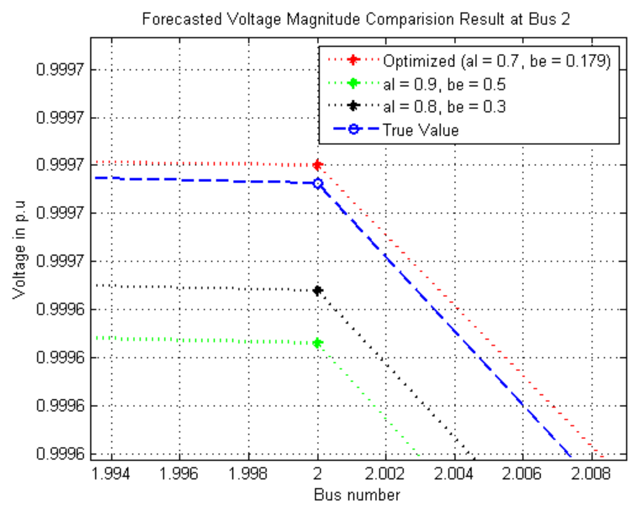

Figure 4-20: Optimized smoothing effect on voltage magnitude forecast at Bus 2

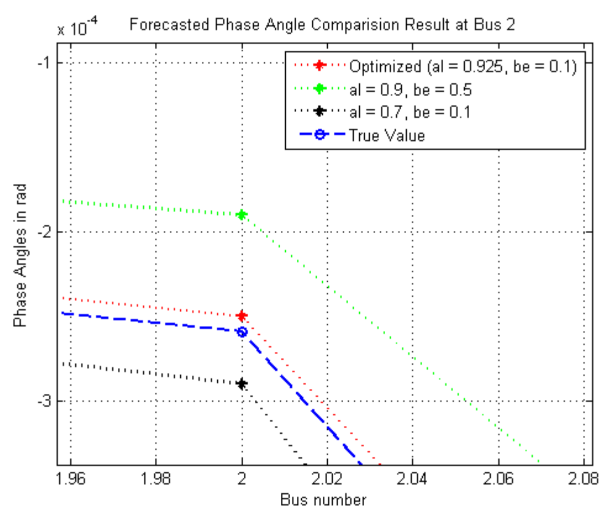

Figure 4-21: Optimized smoothing effect on Phase Angle forecast at Bus 2

4.8 Significance of Optimized Smoothing Parameter in FASE

It is discussed and analyzed FASE so far and confirmed that forecasting is a byproduct of FASE process. This property makes FASE very unique among another state process. Additionally this forecasting of state variables of power system is based on previous data level and trend. So the prediction totally depends on α and β. Optimum values of these smoothing parameter can give a improved forecasting which is very beneficial for power system monitoring, planning, security, and stability. There are some benefits derived from an improved forecasting of system state variables have discussed below:

4.8.1 Substation

- Avoid equipment damage by recognition of problems in future.
- Prevent the outage and thereby improve the continuity of service by advanced monitoring and recording data on the state of a system.
- Defer the construction of new distribution facilities as a result of prior prediction of critical circuit loads.
- Save labor costs by unattended operation of the substation.
- Facilitate the substation engineering and maintenance by forecast data records.

4.8.2 Feeder

- Reduce outage time and revenue losses.
- Release generation and transmission capacity through loss reduction.
- Reduce labor costs by reducing staff responsible for routine and emergency switching operation.
- Facilitate the network engineering and maintenance by forecast data records.

4.8.3 Automatic Meter Reading

- Improve cash flow by faster billing.
- Reduce labor costs by reassigning staff responsible for meter reading.
- Reduce theft by comparison meter reading and forecasted power measurements.

4.8.4 Load Control

- Avoid the damage of distribution transformers and other types of equipment by prior detection of the abnormal diversity of pump loads.
- Reduce distribution losses.
- Prevent overloading problems.

Chapter 5

Conclusions and Future Work

5.1 Conclusions

In upcoming days, it will be a necessary task for a power engineers to efficiently monitor a power system and state estimation is the essential pillar for such task. As so, according to meet perfectly with standard requirements, it needed to be continuously improved. State estimation with forecasting method has been currently pointed out as an eye snatching development.

The main focus of this thesis to validate the forecasting-aided state estimation (FASE) process by comparing with a well-established method as weighted least square (WLS). So it is tried to remained focused in every chapter included in this work. In the second chapter, the implementation aspects of Weighted Least Square (WLS) method is discussed. The mathematical explanation about nonlinear measurement functions, objective functions, Jacobian matrix, gain matrix etc is also discussed. Whole WLS algorithm with sequential steps is shown at the end of this chapter. Forecasting-Aided State Estimation (FASE) process is explained in chapter 3. Since it is our main topic of work, a complete implementation overview with mathematical modeling is described here. Thye contents of this chapter are state forecasting, Kalman filtering stage which is the backbone of FASE algorithm. It is also explained about objective function minimization, Kalman gain calculation. Additionally, the Holt Linear Exponential Smoothing technique which is very important for state forecasting stage. At the of this chapter, different kinds of errors function is discussed which helped us to measure and improve the accuracy of FASE process.

Case study simulation and results is the significant chapter of this thesis work. It illustrates all the implementation results with figures and tables. The necessary implementation outcomes is explained for FASE algorithm particularly the state variables, real and reactive power injections, performance indices etc. The outcomes is very closer to the actual data. It is seen that the forecasting is improving in every iteration and perfectly matched after 50 iteration. Since forecasting is a byproduct of FASE algorthm and it is valuable for advanced system monitoring, it is very good indication to improve it. Moreover, a comparative study with WLS indicates that FASE gives very good results as WLS. However, state estimation using FASE is better than WLS but it is possible to replace WLS with FASE for commercial purpose. Finally, the optimization effect of smoothing parameter on forecasting stage of FASE algorithm is described. Graphically and numerically, it is clearly observed that optimum value of smoothing constant give a very good forecasting of that original value. It is a significant findings of this thesis which can be useful for further development of forecasting-aided state estimation algorithm because state variable forecasting will open the way of efficient power system monitoring, distribution automation and energy management as well.

It can be hope that this thesis can work as a douser of cloud from the sky of FASE development research. The literature review of FASE—representing a history of almost 40 years—has been exhibited in the introduction chapter. Insistence is based on the main functions of FASE (in terms of adequate dynamic modeling, forecasting techniques, and data validation schemes) which can drive it towards the implementation in power system control centers.

5.2 Future Works

The restrictions to the extensive use of the FASE method in the electric power industry have diminished. In researchers opinion, To stimulate future research in FASE, it is necessary to work on the following topic: improvement of forecasting methods; efficient planning for high quality pseudo-measurements; processing of network configuration errors and computational efficiency for large-scale power system applications.

- With respect to forecasting techniques, there is a need for further research on developing prediction method and its optimization with emphasis on their real time applicability. Also, forecasting methods based on nonlinear models. But it is necessary to validate these forecast obtained from nonlinear functions with linear models.

- There is a need of practical experimentation in which we can use the high quality high quality pseudo-measurements generated by a forecasting module. It should be simulated considering real-world situations involving absence of measurements during maintenance services (scheduled or in an emergency) at different redundancy levels. It might be interesting to evaluate how to perpetuate the pseudo-measurements accuracy, since their presence will drive all the SE steps.

- Topology error processing technique to determine the bug in network configuration—via innovation analysis and intelligent systems considered a productive for further research area. We need to find a method for network configuration error from priori state estimation results provided by FASE with low redundancy conditions and/or unobservable network configurations.

- Up to now, there is a lacking of real time implementation of FASE algorithm in small distribution network. It is hoped this condition can drastically change in the near future. Small projects to consolidate FASE as an promising approach would be a good start. Also, given that computational efficiency is vital to the implementation of FASE in large-scale power systems, the computational burden of the introduction of a forecasting step on the SE process should be evaluated. Data debugging process of FASE for large power system is also a important area of research.

In overall conclusion, the SE current status is completely different from what it was three decades ago when power system static SE was developed by Schweppe. It has boost up with the development of greater computing power, efficient statistical models, and more sophisticated approaches to forecast calculation and evaluation. But there is a lot have to be done, with questions still unanswered and new challenges arising, which can give stimulus to FASE future research.

Appendix A

Direct Approach Power Flow Method

The method is based on the DA formulation of the power flow problem. This is a technique, especially designed for radial networks, inspired by well-known backward-forward sweep methods such as Ladder Iterative Technique. DA provides a very compact vectorized formulation with excellent computational and convergence characteristics.

In the application of DA to balanced grids, lines and transformers are modeled as series impedances, z_{ik}, as it is shown in Fig. A.1. The equivalent bus current injection vector, I_g , is calculated from the power injection at each bus, i, given the estimation of the bus voltage vector V at iteration (n) as

$$I_{gi}^{(n)} = \frac{P_i - jQ_i}{conjV_i^{(n)}} \tag{A.1}$$

Assuming a radial grid, the branch current vector can be calculated as

$$B^{(n)} = BIBC.I_g^n \tag{A.2}$$

where BIBC is the so-called bus-injection to branch-current matrix. The entry BIBCbi equals 1 if the current injection of node i contributes to the branch current B_b, and equals 0 otherwise. Finally, a better approximation to the voltage profile can be obtained from

$$\triangle V^{(n+1)} = BCBV.B^n \tag{A.3}$$

where BCBV is the branch-current to bus-voltage matrix. The entry $BCBV_{ib}$ equals the series impedance of branch b if that branch is in the path from node i to the slack bus, and equals 0 otherwise. $\triangle V$ is a vector with the voltage of the slack bus referred to the different bus voltages. An improved approximation to the state variables is subsequently obtained by

$$V^{(n+1)} = V_g - \triangle V^{(n+1)} \tag{A.4}$$

where V_g is a column vector with the slack bus voltage at each entry. Starting from a flat voltage profile, the solution of the distribution power flow is reached by solving (A.1)–(A.4) iteratively up to a specified convergence threshold.

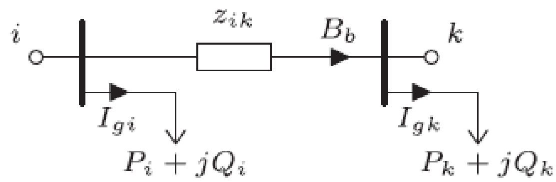

Figure A-1: Basic Diagram for DA Power Flow Method

A brief summary of the changes can be described as:

- Specific branches are selected to break the meshed grid into a radial network. Then, new entries are included in the current injection vector to account for the currents at the selected branches, i.e. $I_g B_{new}$.

- The BIBC matrix is built as in the base case, by considering the currents of the branches used to break the network as additional current injections. However, entries with the value -1 appear now to account for the contribution of the receiving node of the branches used to break the network due to the inverted current reference. Notice that the double-sided contribution of the sending and receiving nodes of a branch used to break the network, Bc, to the current of those branches upstream from the first common parent node, Bb, is null, as they have the same value but opposite references. Additionally, new rows are added to the BIBC matrix with a single non-null entry in order to identify the currents of the branches used to break the network. Taking all this into account the modified BIBC matrix can be obtained as

$$\begin{bmatrix} B \\ B_{new} \end{bmatrix} = BIBC. \begin{bmatrix} I_g \\ B_{new} \end{bmatrix}^{(n)} \tag{A.5}$$

- The BCBV matrix is built as in the base case, but a new row is added for each loop in the grid to account for KVL. The impedances included in the entries of the new rows of the matrix are signed positive or negative according to the reference of the current at the different branches. Then, (A.3) is reformulated as

$$\begin{bmatrix} \triangle V \\ 0 \end{bmatrix}^{(n+1)} = BCBV. \begin{bmatrix} I_g \\ B_{new} \end{bmatrix}^{(n)} \tag{A.6}$$

- By using A.5 and A.6, it can be rewrite as follow

$$\begin{bmatrix} \triangle V \\ 0 \end{bmatrix}^{(n+1)} = BCBV.BIBC \begin{bmatrix} I_g \\ B_{new} \end{bmatrix}^{(n)} = \begin{bmatrix} A & P \\ M & N \end{bmatrix} \begin{bmatrix} I_g \\ B_{new} \end{bmatrix}^{(n)} \tag{A.7}$$

The Application of Kron reduction leads to

$$\triangle V^{(n+1)} = (A - M^T M^{-1} M) I_g^{(n)} \tag{A.8}$$

Bibliography

[1] A. Abur and A. G. Expósito. *Power System State Estimation: Theory and Implementation*. New York: Marcel Decker, 2004.

[2] I. McKenzie Smith. Hughes. *Electrical Technology, Seventh Edition.* Tada McGraw-Hill Publishing Company Limited, 1993.

[3] T Floyed. *Electronic Devices, Fourth Edition.* Prentice Hall International, Inc, 1996.

[4] F. Schweppe and J. Wildes. Power system static state estimation, pt. i: Exact model. *Power Apparatus and Systems, IEEE Transactions on*, PAS-89(1):120–125, Jan 1970.

[5] F. Schweppe and D.B. Rom. Power system static state estimation, pt. ii: Approximation model. *Power Apparatus and Systems, IEEE Transactions on*, PAS-89(1):125–130, Jan 1970.

[6] F. Schweppe. Power system static state estimation, pt. iii: Implementation. *Power Apparatus and Systems, IEEE Transactions on*, PAS-89(1):130–135, Jan 1970.

[7] A. Bose and K. A. Clements. Real-time modeling of power networks. volume 75, page 1607–1622. IEEE, Dec 1987.

[8] B. Stott O. Alsaç, N. Vempati and A. Monticelli. Generalized state estimation. *Power Systems, IEEE Transactions on*, 13(3):1069–1075, Aug 1998.

[9] P. J. Zarco and A. G. Exposito. *Estimacion de estado y deparametros en redes electricas.* Depto. de ingenieria electrica de Sevilla, 1999.

[10] A. S. Debs and R. E. Larson. A dynamic estimator for tracking the state of a power system. *Power Apparatus and System, IEEE Transactions on*, PAS-89:1670–1678, Sep/Oct 1970.

[11] K. Srinivasan and Y. Robichaud. A dynamic estimator for complex bus voltage determination. *Power Apparatus and System, IEEE Transactions on*, PAS-93:1581–1588, Sep/Oct 1974.

[12] M. F. Allam and M. A. Laughton. Power-system dynamic-state estimation by optimal variable incremental displacements. volume 123, page 433–436. IEEE, May 1976.

[13] R. D. Masiello and F. C. Schweppe. A tracking static state estimator. *Power Apparatus and System, IEEE Transactions on*, PAS-90:1025–1033, Mar/Apr 1971.

[14] E. Handschin. Real-time data processing using state estimation in electric power systems. *Real Time Control of Electric Power Systems*, pages 29–57, 1972.

[15] P. A. Cooke D. M. Falcão and A. Brameller. Power system tracking state estimation and bad data processing. *Power Apparatus and System, IEEE Transactions on*, PAS-101:325–333, Feb 1982.

[16] J. Hasegawa . Nishiya, H. Takagi and T. Koike. Dynamic state estimation for electric power systems—introduction of a trend factor and detection of innovation processes. volume 96, pages 79–87. IEEE, May 1976.

[17] J. Hasegawa . Nishiya, H. Takagi and T. Koike. Dynamic state estimation including detection of innovation process for electric power systems. volume 98, pages 52–61. IEEE, Jan 1978.

[18] J. Hasegawa Nishiya, H. Takagi and T. Koike. Dynamic state estimation including anomaly detection and identification for power system. volume 129, pages 192–198. IEEE, Sep 1982.

[19] M. B. Do Coutto Filho A. M. Leite da Silva and J. F. de Queiroz. State forecasting in electric power systems. volume 130, pages 237–244. IEEE, Sep 1983.

[20] M. B. Do Coutto Filho A. M. Leite da Silva and J. M. C. Cantera. An efficient dynamic state estimation including bad data processing. *IEEE transaction on Power System*, 2(4):1050–1058, Nov 1987.

[21] J. M. C. Cantera M. B. Do Coutto Filho, A. M. Leite da Silva and R. A. da Silva. Information debugging for real-time power systems monitoring. volume 36, pages 145–152. IEEE, May 1989.

[22] V. H. Quintana A. P. Alves da Silva and G. K. H. Pang. Solving data acquisition and processing problems in power systems using a pattern analysis approach. volume 138, pages 365–376. IEEE, Jul 1991.

[23] A. P. Alves da Silva and V. H. Quintana. Pattern analysis in power system state estimation. volume 17, pages 51–60. IEEE, Jan 1995.

[24] A. M. Leite da Silva J. C. S. Souza and A. P. Alves da Silva. Information debugging in forecasting-aided state estimation using a pattern analysis approach. volume II, pages 1214–1220. PSCC, ETH, Zurich, Aug 1996.

[25] A. M. Leite da Silva J. C. S. Souza and A. P. Alves da Silva. Data debugging for real-time power system monitoring based on pattern analysis. *IEEE transaction on Power System*, 11(3):1592–1599, Aug 1996.

[26] A. M. Leite da Silva J. C. S. Souza and A. P. Alves da Silva. Data visualization and identification of anomalies in power system state estimation using artificial neural networks. volume 144, pages 445–455. IEEE, Sep 1998.

[27] A. M. Leite da Silva J. C. S. Souza and A. P. Alves da Silva. Online topology determination and bad data suppression in power system operation using artificial neural networks. *IEEE transaction on Power System*, 13(3):796–803, Aug 1998.

[28] K. R. Shih and S. J. Huang. Application of a robust algorithm for dynamic state estimation of a power system. *IEEE transaction on Power System*, 17(1):141–147, Feb 2002.

[29] S. J. Huang and K. R. Shih. Dynamic state estimation scheme including nonlinear measurement function considerations. volume 149, pages 673–678. IEEE, Nov 2002.

[30] S. J. Huang J. M. Lin and K. R. Shih. Application of sliding surface- enhanced control for dynamic state estimation of a power system. *IEEE transaction on Power System*, 18(2):570–577, May 2003.

[31] S. J. Huang and J. M. Lin. Enhancement of anomalous data mining in power system predicting-aided state estimation. *IEEE transaction on Power System*, 19(1):610–619, Feb 2004.

[32] C. Y. Evrenosoglu M. Hassanzadeh. A regression-based analysis based state transition model for power system dynamic state estimation. pages 1–5. IEEE, Sep 2012.

[33] Z. Y. Huang K. Kalsi R. S. Diao K. K Anderson Y. L. Li Y. N. Sun, P. W. Du. Pmu placement for dynamic state tracking of power systems. pages 1–7. IEEE, Aug 2011.

[34] G. J. Cokkinides A. P. Meliopoulos E. Farantatos, G.K. Stefopoulos. Pmu-based dynamic state estimation for electric power systems. pages 1–8. IEEE, Jul 2009.

[35] N. R. Shivakumar A. Jain. Use of pmu in dynamic state estimation of power systems. pages 1–8. IEEE, Sep 2009.

[36] S. J. Huang K. R. Shih. Application of a robust algorithm for dynamic state estimation of a power system. *IEEE transaction on Power System*, 17(1):141–147, Feb 2002.

[37] M. L. Scala J. B. Zhao, G. X. Zhang. Pmu based robust dynamic state estimation method for power systems. pages 26–30. IEEE, Jul 2015.

[38] K. Das Ge. N. Korres N. M. Manousakis A. K. Sinha Z. Y. He J. B. Zhao, G. X. Zhang. Power system real-time monitoring by using pmu-based robust state estimation method. *IEEE transaction on Smart Grid*, 7(1):300–309, Jan 2016.

[39] V. Terzija G. Valverde, A. T. Saric. Stochastic monitoring of distribution networks including correlated input variables. *IEEE transaction on Power System*, 28(1):246–255, Feb 2015.

[40] M. Ilic E. Blood, B. Krogh. Electric power system static state estimation through kalman filtering and load forecasting. pages 1–6. IEEE, Jul 2008.

[41] B. Stott and O. Alsac. Fast decoupled load flow. *IEEE Transactions on Power Apparatus and Systems*, PAS-93(3):859–869, May 1974.

[42] S. J. Huang and K. R. Shih. Dynamic-state-estimation scheme including nonlinear measurement-function considerations. *IEE Proceedings - Generation, Transmission and Distribution*, 149(6):673–678, Nov 2002.

[43] M. B. Do Coutto Filho, J. C. Stacchini de Souza, and R. S. Freund. Forecasting-aided state estimation x2014;part ii: Implementation. *IEEE Transactions on Power Systems*, 24(4):1678–1685, Nov 2009.

[44] Kisang Ryu and Alfonso Sanchez. The evaluation of forecasting methods at an institutional foodservice dining facility. *The Journal of Hospitality Financial Management*, 11(1):27–45, 2003.

[45] José M. Cano, Md. Rejwanur R. Mojumdar, Joaquín G. Norniella, and Gonzalo A.Orcajo. Phase shifting transformer model for direct approach power flow studies. *International Journal of Electrical Power & Energy Systems,* 91:71 – 79, 2017.